



HAL
open science

Three-dimensional elastic solutions for functionally graded circular plates

Roberta Sburlati, Lorenzo Bardella

► **To cite this version:**

Roberta Sburlati, Lorenzo Bardella. Three-dimensional elastic solutions for functionally graded circular plates. *European Journal of Mechanics - A/Solids*, 2011, 10.1016/j.euromechsol.2010.12.008 . hal-00734537

HAL Id: hal-00734537

<https://hal.science/hal-00734537>

Submitted on 23 Sep 2012

HAL is a multi-disciplinary open access archive for the deposit and dissemination of scientific research documents, whether they are published or not. The documents may come from teaching and research institutions in France or abroad, or from public or private research centers.

L'archive ouverte pluridisciplinaire **HAL**, est destinée au dépôt et à la diffusion de documents scientifiques de niveau recherche, publiés ou non, émanant des établissements d'enseignement et de recherche français ou étrangers, des laboratoires publics ou privés.

Accepted Manuscript

Title: Three-dimensional elastic solutions for functionally graded circular plates

Authors: Roberta Sburlati, Lorenzo Bardella

PII: S0997-7538(10)00146-4

DOI: [10.1016/j.euromechsol.2010.12.008](https://doi.org/10.1016/j.euromechsol.2010.12.008)

Reference: EJMSOL 2663

To appear in: *European Journal of Mechanics / A Solids*

Received Date: 17 September 2010

Revised Date: 20 December 2010

Accepted Date: 21 December 2010

Please cite this article as: Sburlati, R., Bardella, L. Three-dimensional elastic solutions for functionally graded circular plates, *European Journal of Mechanics / A Solids* (2010), doi: 10.1016/j.euromechsol.2010.12.008

This is a PDF file of an unedited manuscript that has been accepted for publication. As a service to our customers we are providing this early version of the manuscript. The manuscript will undergo copyediting, typesetting, and review of the resulting proof before it is published in its final form. Please note that during the production process errors may be discovered which could affect the content, and all legal disclaimers that apply to the journal pertain.



Three-dimensional elastic solutions for functionally graded circular plates

Roberta Sburlati^a and Lorenzo Bardella^{b*}

^a*DICAT, University of Genova
Via Montallegro, 1 — 16145 Genova, Italy*

^b*DICATA, University of Brescia
Via Branze, 43 — 25123 Brescia, Italy*

Dedicated to the memory of Professor Osvaldo De Donato

December 20, 2010

Abstract

Three-dimensional elastic solutions are obtained for a functionally graded thick circular plate subject to axisymmetric conditions. We consider an isotropic material where the Young modulus depends exponentially on the position along the thickness, while the Poisson ratio is constant. The solution method utilises a Plevako's representation form which reduces the problem to the construction of a potential function satisfying a linear fourth-order partial differential equation. We write this potential function in terms of Bessel functions and we *pointwise* assign mixed boundary conditions. The analytic solution is obtained in a general form and explicitly presented by assuming transversal load on the upper face and zero displacements on the mantle; this is done by superposing the solutions of problems with suitably imposed radial displacement. We validate the solution by means of a finite element approach; in this way, we highlight the effects of the material inhomogeneity and the limits of the employed numerical method near the mantle, where the solution shows a large sensitivity to the boundary conditions.

Keywords: Functionally graded plates; Boundary value problems; Finite element method

*Corresponding author: Tel.: +39-030-3711238; fax: +39-030-3711312. *E-mail address:* lorenzo.bardella@ing.unibs.it

1 Introduction

Functionally graded materials (FGMs) are composites inhomogeneous at the macroscopic scale because of the continuous spatial variation of the volume fractions of their constituent homogeneous phases. If the characteristic length scale of such variation is much larger than the size of the microstructural elements (reinforcements, voids, etc.), it is possible to describe the behaviour of each macroscopic material point by means of its relevant effective properties obtained via standard homogenisation techniques for statistically homogeneous aggregates. Instead, care must be taken in estimating the effective properties within regions where the microstructure varies rapidly (see, e.g., Reiter *et al.* 1997; Yin *et al.* 2004).

FGMs were initially developed for high temperature applications to avoid detachments in laminated composites due to their typical abrupt change of the material properties. The advantage of smoothing the mismatch in materials properties makes FGMs very useful for various applications in which the structure is subjected to extreme conditions (Suresh 2001). One of their most relevant advantages, with respect to conventional laminated composites, concerns the scarce relevance in FGMs of structural integrity issues such as delamination or fracture (e.g., Vel and Batra 2003; Erdogan 1995).

The modelling of FGMs is currently an active research area and, over the years, different approaches have been introduced to investigate on the mechanical performance of FGM structures (plates and coatings). Some problems have been studied by using the inhomogeneous elasticity theory but, because of the inherent mathematical difficulties, much of the work has been carried out by using numerical methods (Reddy *et al.* 1999; Reddy 2000; Reddy and Cheng 2001; Ma and Wang 2004).

Recently, some investigators presented three-dimensional analytic solutions for the bending of FGM plates subject to transversal loads by assuming specific boundary conditions on the mantle for the description of either simply supported or clamped plates (e.g., Li *et al.* 2008; Kashtalyan 2004). The limit of these 3D solutions consists in the fact that the boundary conditions are satisfied on the mantle only in some average sense, not *pointwise*.

In this paper, we develop a method, within the framework of the linear inhomogeneous elasticity theory, to find analytic solutions for FGM cylindrical bodies subject to axisymmetric boundary conditions. The solution is explicitly found in the case a right cylinder of modest thickness subject to axisymmetric transversal loads with mixed boundary conditions (plate-like body), with particular reference to the case of zero displacement components on the mantle. We adopt a commonly used model for the material gradation: a spatially uniform Poisson's ratio and an exponential variation along the thickness coordinate z for the Young modulus (see, e.g., Erdogan 1995; Kashtalyan 2004). This choice of gradation has been made by Martin *et al.* (2002) and Chan *et al.* (2004) for solving elastic problems by means of the boundary element method.

The analytic solution is constructed by introducing a potential function leading to a fourth-order linear partial differential equation (Plevako 1971). Furthermore, we write the potential function with a Bessel expansion with respect to the radial coordinate r and, in this way, the solution consists of four series of coefficients and two functions of z completely

determined by the boundary conditions (Sburlati 2009).

We validate the analytic solution by means of a comparison with a finite element analysis. Also, we show in detail the effects of the material inhomogeneity with particular reference to the mantle, where it turns out that the solution provided by the finite element method (FEM) may be quite inaccurate, while the analytic solution is obtained in a closed form. The chosen benchmark might be useful to evaluate the accuracy of numerical or approximate analytic approaches (see, e.g., Elishakoff and Gentilini 2005).

2 Formulation of the problem

In figure 1, on the left, we show a sketch of the problem under investigation. We use a cylindrical coordinate system $(0; r, \vartheta, z)$ to describe the elastic field in a cylinder made up of an isotropic FGM with Young's modulus $E = E(z)$ varying only along the z -direction, while the Poisson ratio ν is spatially uniform and positive; b denotes the radius of the cylinder and h its thickness. We suppose that the applied loads on the upper face and the boundary conditions are axisymmetric; consequently, the circumferential displacement component is zero and the radial and transversal components of the displacement, say u and w respectively, are functions of r and z only. By considering null body forces, the elasticity equations assume the form (Plevako 1971):

$$\begin{aligned} \nabla^2 u - \frac{u}{r^2} + \frac{1}{1-2\nu} \frac{\partial \Theta}{\partial r} + \left(\frac{\partial u}{\partial z} + \frac{\partial w}{\partial r} \right) \frac{1}{E(z)} \frac{d}{dz} E(z) &= 0, \\ \nabla^2 w + \frac{1}{1-2\nu} \frac{\partial \Theta}{\partial z} + \left(\frac{\partial w}{\partial z} + \frac{\nu}{1-2\nu} \Theta \right) \frac{2}{E(z)} \frac{d}{dz} E(z) &= 0, \end{aligned} \quad (2.1)$$

where

$$\Theta = \frac{\partial u}{\partial r} + \frac{u}{r} + \frac{\partial w}{\partial z}.$$

The body is subjected to transverse compressive loading $p(r)$ on its upper face ($z = 0$), so the boundary conditions on the ends are

$$\sigma_z(r, 0) = -p(r), \quad \sigma_z(r, h) = 0, \quad \tau_{rz}(r, 0) = 0, \quad \tau_{rz}(r, h) = 0. \quad (2.2)$$

On the mantle ($r = b$) we impose vanishing displacements:

$$w(b, z) = 0, \quad u(b, z) = 0. \quad (2.3)$$

The elastic problem is consistent with the notion of clamped edge within the classical bending plate theory (Love 1927).

3 The solution technique

To find the analytic solution we follow the Plevako (1971) approach in which the displacement field, in the axisymmetric case, is expressed in terms of a potential function $L = L(r, z)$, in

the form

$$u = -\frac{1+\nu}{E(z)} \frac{\partial}{\partial r} \left(\nu \nabla_r^2 L - (1-\nu) \frac{\partial^2}{\partial z^2} L \right),$$

$$w = -\frac{2(1+\nu)}{E(z)} \frac{\partial}{\partial z} \nabla_r^2 L + (1+\nu) \frac{\partial}{\partial z} \left[\frac{1}{E(z)} \left(\nu \nabla_r^2 L - (1-\nu) \frac{\partial^2}{\partial z^2} L \right) \right],$$

where ∇_r^2 is the radial Laplace operator; $L(r, z)$ satisfies the Plevako equation

$$\nabla^2 \left(\frac{1}{E(z)} \nabla^2 L \right) - \frac{1}{1-\nu} \nabla_r^2 L \frac{d^2}{dz^2} \frac{1}{E(z)} = 0. \quad (3.1)$$

The stress field reads:

$$\sigma_r = \frac{\nu}{r} \frac{\partial}{\partial r} \nabla_r^2 L + \frac{\partial^2}{\partial z^2} \nabla_r^2 L - \frac{1-\nu}{r} \frac{\partial^3}{\partial r \partial z^2} L, \quad \sigma_z = \nabla_r^4 L, \quad (3.2)$$

$$\sigma_\vartheta = \nu \nabla_r^4 L - \frac{\nu}{r} \frac{\partial}{\partial r} \nabla_r^2 L + \nu \frac{\partial^2}{\partial z^2} \nabla_r^2 L + \frac{1-\nu}{r} \frac{\partial^3}{\partial r \partial z^2} L, \quad \tau_{rz} = -\frac{\partial^2}{\partial r \partial z} \nabla_r^2 L.$$

By using these equations it is easy to show that

$$\sigma_\vartheta - \nu(\sigma_r + \sigma_z) = E(z) \frac{u}{r}.$$

Now we introduce an exponential function describing the Young's modulus variation:

$$E(z) = E_0 e^{2kz} \quad \text{with} \quad k = \frac{1}{2h} \ln \left(\frac{E_h}{E_0} \right), \quad (3.3)$$

where $E_0 = E(0)$ and $E_h = E(h)$. By using the position (3.3), we write equation (3.1) as

$$\nabla_r^4 L + 2 \left(\frac{\partial^2}{\partial z^2} - 2k \frac{\partial}{\partial z} - 2k^2 \frac{\nu}{1-\nu} \right) \nabla_r^2 L + \left(\frac{\partial^2}{\partial z^2} - 4k \frac{\partial}{\partial z} + 4k^2 \right) \frac{\partial^2}{\partial z^2} L = 0. \quad (3.4)$$

We remark that this equation becomes biharmonic in the case of homogeneous material.

In order to construct the explicit solution for equation (3.4), we write the function $L(r, z) - L(b, z)$, clearly vanishing for $r = b$, in terms of a Bessel expansion with respect to r (Sneddon 1966; Watson 1966). By defining

$$\beta(z) = L(b, z), \quad (3.5)$$

we set

$$L(r, z) = \beta(z) + \sum_{j=1}^{\infty} L_j(z) J_0(\phi_j r), \quad \text{where} \quad \phi_j = \frac{z_j^0}{b}$$

and z_j^0 , for $j = 1, 2, 3, \dots$, are the positive roots of $J_0(x)$, the zero-order Bessel function; the functions $L_j(z)$ are

$$L_j(z) = \frac{2}{[b J_1(\phi_j b)]^2} \int_0^b [L(\rho, z) - \beta(z)] J_0(\phi_j \rho) \rho d\rho,$$

where $J_1(x)$ is the first-order Bessel function. After introducing the functions

$$\alpha(z) = \nabla_r^2 L(r, z) \Big|_{r=b} \quad \text{and} \quad \gamma(z) = \nabla_r^4 L(r, z) \Big|_{r=b} \quad (3.6)$$

we obtain (Sburlati 2009):

$$\nabla_r^2 L(r, z) = \alpha(z) - \sum_{j=1}^{\infty} \left(\phi_j^2 L_j(z) + 2 \frac{\alpha(z)}{\phi_j b J_1(\phi_j b)} \right) J_0(\phi_j r), \quad (3.7)$$

and

$$\nabla_r^4 L(r, z) = \gamma(z) - \sum_{j=1}^{\infty} \left(\phi_j^4 L_j(z) + 2 \frac{\gamma(z) - \phi_j^2 \alpha(z)}{\phi_j b J_1(\phi_j b)} \right) J_0(\phi_j r). \quad (3.8)$$

By substituting expressions (3.7) and (3.8) in equation (3.4), one has

$$\begin{aligned} & \sum_{j=1}^{\infty} \left[L_j''''(z) - 4k L_j'''(z) + (4k^2 - 2\phi_j^2) L_j''(z) + 4\phi_j^2 k L_j'(z) + \phi_j^2 (4k^2 \omega^2 + \phi_j^2) L_j(z) \right. \\ & \quad \left. - \left(4\alpha''(z) - 8k\alpha'(z) - 2\alpha(z)(4k^2 \omega^2 + \phi_j^2) + 2\gamma(z) \right) \frac{1}{\phi_j b J_1(\phi_j b)} \right] J_0(\phi_j r) \\ & \quad + \beta_j''''(z) - 4k\beta_j'''(z) + 4k^2\beta_j''(z) + 2\alpha''(z) - 4k\alpha'(z) - 4k^2\omega^2\alpha(z) + \gamma(z) = 0 \end{aligned} \quad (3.9)$$

where prime denotes the derivative with respect to z and $\omega^2 = \nu/(1-\nu)$. Now, by evaluating equation (3.9) at $r = b$, we get

$$\gamma(z) = -\beta_j''''(z) + 4k\beta_j'''(z) - 4k^2\beta_j''(z) - 2\alpha''(z) + 4k\alpha'(z) + 4k^2\omega^2\alpha(z). \quad (3.10)$$

By using this result in equation (3.9), we obtain

$$\begin{aligned} & L_j''''(z) - 4k L_j'''(z) + (4k^2 - 2\phi_j^2) L_j''(z) + 4\phi_j^2 k L_j'(z) \\ & \quad + \phi_j^2 (4k^2 \omega^2 + \phi_j^2) L_j(z) + F_j(z) = 0, \end{aligned} \quad (3.11)$$

where

$$F_j(z) = 2 \frac{\beta_j''''(z) - 4k\beta_j'''(z) + 4k^2\beta_j''(z) + \phi_j^2\alpha(z)}{\phi_j b J_1(\phi_j b)}. \quad (3.12)$$

We write the solution of (3.11) in the form

$$L_j(z) = L_j^0(z) + L_j^1(z),$$

where

$$\begin{aligned} L_j^0(z) = e^{kz} & \left[e^{\beta_j z} \left(A_j \cos(\alpha_j z) + B_j \sin(\alpha_j z) \right) \right. \\ & \left. + e^{-\beta_j z} \left(C_j \cos(\alpha_j z) + D_j \sin(\alpha_j z) \right) \right] \end{aligned} \quad (3.13)$$

and

$$L_j^1(z) = \frac{e^{kz} F_j(z) R_j(z)}{k\omega (\alpha_j^2 + \beta_j^2) \phi_j^2 b J_1(\phi_j b)}. \quad (3.14)$$

We have set

$$\begin{aligned} R_j(z) = \int_0^z e^{-k\zeta} \alpha(\zeta) & \left[\beta_j \cosh[\alpha_j(\zeta - z)] \sin[\alpha_j(\zeta - z)] \right. \\ & \left. - \alpha_j \sinh[\beta_j(\zeta - z)] \cos[\beta_j(\zeta - z)] \right] d\zeta \end{aligned} \quad (3.15)$$

where the real parameters α_j and β_j are

$$\alpha_j = \frac{\sqrt{2}}{2} \sqrt{\sqrt{k^4 + \phi_j^4 + 2k^2\phi_j^2(2\omega^2 + 1)} - k^2 - \phi_j^2} \quad \text{and} \quad \beta_j = \frac{k\omega\phi_j}{\alpha_j}.$$

This allows us to write the solution of equation (3.9) as

$$L(r, z) = L^0(r, z) + L^1(r, z), \quad (3.16)$$

where

$$L^0(r, z) = \sum_{j=1}^{\infty} L_j^0(z) J_0(\phi_j r), \quad (3.17)$$

$$L^1(r, z) = \beta(z) + \sum_{j=1}^{\infty} L_j^1(z) J_0(\phi_j r). \quad (3.18)$$

Hence, the displacement field assumes the form

$$u(r, z) = e^{-2kz} \sum_{j=1}^{\infty} (u_j^0(z) + u_j^1(z)) J_1(\phi_j r), \quad (3.19)$$

where

$$\begin{aligned} u_j^0(z) &= -\frac{1-\nu^2}{E_0} \phi_j \left(L_j^{0''}(z) + \omega^2 \phi_j^2 L_j^0(z) \right), \\ u_j^1(z) &= -\frac{1-\nu^2}{E_0} \phi_j \left(L_j^{1''}(z) + \omega^2 \phi_j^2 L_j^1(z) + \frac{2\omega^2 \alpha(z)}{b \phi_j J_1(\phi_j b)} \right), \end{aligned}$$

and

$$\begin{aligned} w(r, z) &= e^{-2kz} \sum_{j=1}^{\infty} (w_j^0(z) + w_j^1(z)) J_0(\phi_j r) \\ &\quad - (1-\nu) e^{-2kz} \left(\beta'''(z) - 2k\beta''(z) + (2+\omega^2)\alpha'(z) + 2\omega^2 k\alpha(z) \right), \quad (3.20) \end{aligned}$$

where

$$\begin{aligned} w_j^0(z) &= -\frac{1-\nu^2}{E_0} \left(L_j^{0''''}(z) - 2kL_j^{0'''}(z) - (2+\omega^2)\phi_j^2 L_j^{0'}(z) - 2\omega^2 k\phi_j^2 L_j^0(z) \right), \\ w_j^1(z) &= -\frac{1-\nu^2}{E_0} \left(L_j^{1''''}(z) - 2kL_j^{1'''(z)} - (2+\omega^2)\phi_j^2 L_j^{1'}(z) - 2\omega^2 k\phi_j^2 L_j^1(z) \right) \\ &\quad + \frac{2(1-\nu^2)}{E_0 b \phi_j J_1(\phi_j b)} \left((2+\omega^2)\alpha'(z) + 2\omega^2 k\alpha(z) \right). \end{aligned}$$

Now, we evaluate the stress components:

$$\begin{aligned} \sigma_r(r, z) &= \sum_{j=1}^{\infty} \left(\sigma_{r(j)}^0(z) + \sigma_{r(j)}^1(z) \right) J_0(\phi_j r) \\ &\quad + \sum_{j=1}^{\infty} \left(\bar{\sigma}_{r(j)}^0(z) + \bar{\sigma}_{r(j)}^1(z) \right) \frac{J_1(\phi_j r)}{r} + \alpha''(z), \quad (3.21) \end{aligned}$$

where

$$\begin{aligned}\sigma_{r(j)}^0(z) &= -\phi_j^2 L_j^{0''}(z), & \sigma_{r(j)}^1(z) &= -\phi_j^2 L_j^{1''}(z) - \frac{2}{b\phi_j J_1(\phi_j b)} \alpha''(z), \\ \bar{\sigma}_{r(j)}^0(z) &= (1-\nu) \phi_j \left(L_j^{0''}(z) + \omega^2 \phi_j^2 L_j^0(z) \right), \\ \bar{\sigma}_{r(j)}^1(z) &= (1-\nu) \phi_j \left(L_j^{1''}(z) + \omega^2 \phi_j^2 L_j^1(z) + \frac{2\omega^2 \alpha(z)}{b\phi_j J_1(\phi_j b)} \right); \end{aligned}$$

$$\begin{aligned}\sigma_{\vartheta}(r, z) &= \sum_{j=1}^{\infty} \left(\sigma_{\vartheta(j)}^0(z) + \sigma_{\vartheta(j)}^1(z) \right) J_0(\phi_j r) \\ &\quad + \sum_{j=1}^{\infty} \left(\bar{\sigma}_{\vartheta(j)}^0(z) + \bar{\sigma}_{\vartheta(j)}^1(z) \right) \frac{J_1(\phi_j r)}{r} + \nu \left(\alpha''(z) + \gamma(z) \right), \quad (3.22)\end{aligned}$$

where $\gamma(z)$ is given by (3.10) and

$$\begin{aligned}\sigma_{\vartheta(j)}^0(z) &= -\nu \phi_j^2 \left(L_j^{0''}(z) - \phi_j^2 L_j^0(z) \right), \\ \sigma_{\vartheta(j)}^1(z) &= -\nu \phi_j^2 \left(L_j^{1''}(z) - \phi_j^2 L_j^1(z) \right) - \frac{2\nu}{b\phi_j J_1(\phi_j b)} \left(\gamma(z) + \alpha''(z) - \phi_j^2 \alpha(z) \right), \\ \bar{\sigma}_{\vartheta(j)}^0(z) &= -\bar{\sigma}_{r(j)}^0(z), & \bar{\sigma}_{\vartheta(j)}^1(z) &= -\bar{\sigma}_{r(j)}^1(z); \\ \sigma_z(r, z) &= \sum_{j=1}^{\infty} \left(\sigma_{z(j)}^0(z) + \sigma_{z(j)}^1(z) \right) J_0(\phi_j r) + \gamma(z), \quad (3.23)\end{aligned}$$

where

$$\begin{aligned}\sigma_{z(j)}^0(z) &= \phi_j^4 L_j^0(z), & \sigma_{z(j)}^1(z) &= \phi_j^4 L_j^1(z) + \frac{2}{b\phi_j J_1(\phi_j b)} (\phi_j^2 \alpha(z) - \gamma(z)); \\ \tau_{rz}(r, z) &= \sum_{j=1}^{\infty} \left(\tau_{rz(j)}^0(z) + \tau_{rz(j)}^1(z) \right) J_1(\phi_j r), \quad (3.24)\end{aligned}$$

where

$$\tau_{rz(j)}^0(z) = -\phi_j^3 L_j^{0'}(z), \quad \tau_{rz(j)}^1(z) = -\phi_j^3 L_j^{1'}(z) - \frac{2}{bJ_1(\phi_j b)} \alpha'(z).$$

Furthermore, we write the following stress components as:

$$\sigma_z^0(r, z) = \sum_{j=1}^{\infty} \sigma_{z(j)}^0(z) J_0(\phi_j r), \quad \tau_{rz}^0(r, z) = \sum_{j=1}^{\infty} \tau_{rz(j)}^0(z) J_1(\phi_j r), \quad (3.25)$$

where the shear stress is written in terms of a Dini expansion.¹

The determination of the explicit solution (3.19)–(3.24) requires the prescription of the boundary conditions in order to evaluate the four series of coefficients A_j, B_j, C_j, D_j of (3.13) and the functions $\alpha(z)$ and $\beta(z)$ of (3.14) and (3.12).

¹For any detail on Dini expansions we refer to Watson (1966). Here we recall that, by using the symbols of page 597, by putting $\nu = H = 1$ and rescaling the radius from 1 to b , we see that a continuous function $f(r)$ can be written in terms of the following Dini expansion: $f(r) = \sum_{k=1}^{\infty} c_k J_1(\phi_k r)$ where $c_k = 2 \int_0^b r f(r) J_1(\phi_k r) dr / [b J_1(\phi_k b)]^2$.

We remark that, in order to check the axisymmetric conditions: $\lim_{r \rightarrow 0} \sigma_r(r, z) = \lim_{r \rightarrow 0} \sigma_\vartheta(r, z)$ and $\tau_{rz}(0, z) = 0$, we use equations (3.21), (3.22), and (3.24) and exploit the relation:

$$\sum_{j=1}^{\infty} \frac{2 J_0(\phi_j r)}{b \phi_j J_1(\phi_j b)} = 1$$

which is true for $r < b$ (Watson 1966).

4 Analysis of the boundary conditions

In this section we impose the boundary conditions (2.2)–(2.3) to determine the explicit solution. First of all, we notice that, for the subclass of solutions where $w(b, z) = 0$, by (3.20), we have

$$\beta'''(z) - 2k\beta''(z) + (2 + \omega^2)\alpha'(z) + 2k\omega^2\alpha(z) = 0. \quad (4.1)$$

Further, since also $u(b, z) = 0$, the following relations

$$\begin{aligned} \sigma_r(b, z) &= \alpha''(z), & \sigma_z(b, z) &= \gamma(z) = \omega^2 \alpha''(z), \\ \sigma_\vartheta(b, z) &= \nu[\gamma(z) + \alpha''(z)] = \omega^2 \alpha''(z). \end{aligned} \quad (4.2)$$

can be obtained by using (3.21), (3.22), (3.23), and (3.19).

Now, we obtain the solution of the problem of section 2 as superposition of the solutions of the two new problems A and B represented in figure 1. More precisely, we first define a problem A by assuming $\alpha(z) = 0$ and $\beta(z) = 0$ in order to reduce the solution of equation (3.4) to the sole contribution $L^0(r, z)$. In this way, we obtain the coefficients A_j, B_j, C_j, D_j by using the boundary conditions on the stress (2.2); the condition $w(b, z) = 0$ is automatically verified while, the radial displacement $u^A(b, z)$ (where the superscript A refers to the problem A) is obtained from (3.19). The solution of problem A gives so rise to an infinite sum of terms, each of them generating displacement fields $w(r, z)$ and $u(r, z)$ satisfying the so called semi-inverse Levinson assumptions defined in Levinson (1985) and generalized, for cross section of arbitrary shape, in Nicotra *et al.* (1999). Hence, we define the problem B with the following boundary conditions: free loading ends, $w^B(b, z) = 0$ and $u^B(b, z) = -u^A(b, z)$; these conditions imply $\alpha(z) \neq 0$ and $\beta(z)$ obtained by (4.1).

4.1 Problem A

We now consider the subclass of elastic solutions in which

$$\alpha(z) = 0, \quad \beta(z) = 0, \quad (4.3)$$

$$\sigma_z^A(r, 0) = -p(r), \quad \sigma_z^A(r, h) = 0, \quad \tau_{rz}^A(r, 0) = 0, \quad \tau_{rz}^A(r, h) = 0. \quad (4.4)$$

The condition $w^A(b, z) = 0$ is automatically satisfied because of the restrictions (4.3) (see equation (3.20)).

The solution of equation (3.9), with the position (4.3), becomes

$$L^A(r, z) = \sum_{j=1}^{\infty} L_j^A(z) J_0(\phi_j r),$$

where

$$L_j^A(z) = e^{kz} \left[e^{\beta_j z} [A_j \cos(\alpha_j z) + B_j \sin(\alpha_j z)] + e^{-\beta_j z} [C_j \cos(\alpha_j z) + D_j \sin(\alpha_j z)] \right]. \quad (4.5)$$

Now, we write the load applied on the upper face as a Bessel expansion

$$p(r) = \sum_{j=1}^{\infty} p_j J_0(\phi_j r), \quad \text{where} \quad p_j = \frac{2}{[b J_1(\phi_j b)]^2} \int_0^b p(\rho) J_0(\phi_j \rho) d\rho, \quad (4.6)$$

by assuming, for simplicity, $p(b) = 0$. By virtue of conditions (4.4) we have

$$L_j^A(0) = \frac{p_j}{\phi_j^4}, \quad \frac{d}{dz} L_j^A(z) \Big|_{z=0} = 0, \quad L_j^A(h) = 0, \quad \frac{d}{dz} L_j^A(z) \Big|_{z=h} = 0,$$

which lead to the following expressions of the coefficients of (4.5):

$$\begin{aligned} A_j &= -\frac{p_j}{H_j} \left[e^{2h\beta_j} \left[\beta_j (k - \beta_j) (1 - \cos(2h\alpha_j)) - \alpha_j \beta_j \sin(2h\alpha_j) \right] + \alpha_j^2 (1 - e^{2h\beta_j}) \right], \\ B_j &= -\frac{p_j}{H_j} \left[e^{2h\beta_j} \left(\alpha_j \beta_j \cos(2h\alpha_j) - \beta_j (k - \beta_j) \sin(2h\alpha_j) \right) - \alpha_j \beta_j - k \alpha_j (1 - e^{2h\beta_j}) \right], \\ C_j &= -\frac{p_j}{H_j} e^{2h\beta_j} \left[\alpha_j \beta_j \sin(2h\alpha_j) - \beta_j (k + \beta_j) (1 - \cos(2h\alpha_j)) - \alpha_j^2 (1 - e^{2h\beta_j}) \right], \\ D_j &= -\frac{p_j}{H_j} e^{2h\beta_j} \left[e^{2h\beta_j} \alpha_j \beta_j - \alpha_j \beta_j \cos(2h\alpha_j) + \beta_j (k + \beta_j) \sin(2h\alpha_j) + k \alpha_j (1 - e^{2h\beta_j}) \right] \end{aligned}$$

where

$$H_j = \phi_j^4 \left[\alpha_j^2 (1 - e^{2h\beta_j})^2 - 2\beta_j^2 e^{2h\beta_j} (1 - \cos(2h\alpha_j)) \right].$$

By (3.19) and (3.20), the displacement components assume the form

$$u^A(r, z) = -\frac{1 - \nu^2}{E_0} e^{-2kz} \sum_{j=1}^{\infty} \phi_j \left(L_j^{A''}(z) + \omega^2 \phi_j^2 L_j^A(z) \right) J_1(\phi_j r), \quad (4.7)$$

$$\begin{aligned} w^A(r, z) &= -\frac{1 - \nu^2}{E_0} e^{-2kz} \sum_{j=1}^{\infty} \left(L_j^{A''''}(z) - 2k L_j^{A''}(z) \right. \\ &\quad \left. - (2 + \omega^2) \phi_j^2 L_j^{A'}(z) - 2\omega^2 k \phi_j^2 L_j^A(z) \right) J_0(\phi_j r). \quad (4.8) \end{aligned}$$

and, by (3.21)–(3.24), the stress components are

$$\sigma_r^A(r, z) = - \sum_{j=1}^{\infty} \phi_j^2 L_j^{A''}(z) J_0(\phi_j r) + (1 - \nu) \sum_{j=1}^{\infty} \phi_j \left(L_j^{A''}(z) + \omega^2 \phi_j^2 L_j^A(z) \right) \frac{J_1(\phi_j r)}{r}, \quad (4.9)$$

$$\begin{aligned} \sigma_{\vartheta}^A(r, z) = & -\nu \sum_{j=1}^{\infty} \phi_j^2 \left(L_j^{A''}(z) - \phi_j^2 L_j^A(z) \right) J_0(\phi_j r) \\ & - (1 - \nu) \sum_{j=1}^{\infty} \phi_j \left(L_j^{A''}(z) + \omega^2 \phi_j^2 L_j^A(z) \right) \frac{J_1(\phi_j r)}{r}, \end{aligned} \quad (4.10)$$

$$\sigma_z^A(r, z) = \sum_{j=1}^{\infty} \phi_j^4 L_j^A(z) J_0(\phi_j r), \quad \tau_{rz}^A(r, z) = - \sum_{j=1}^{\infty} \phi_j^3 L_j^{A'}(z) J_1(\phi_j r). \quad (4.11)$$

Note that a combination of equations (4.9), (4.10), and (4.7) furnishes

$$\sigma_r^A(b, z) = -\sigma_{\vartheta}^A(b, z) = -\frac{E_0 e^{2kz}}{b(1 + \nu)} u^A(b, z), \quad (4.12)$$

which implies that σ_r^A , σ_{ϑ}^A , and u^A vanish in the same point on the mantle. An analysis of the previous expressions shows that, for $r = b$, each term of the expansion of (4.7) vanishes for a value of z , say s , obtained by solving the following transcendental equations

$$L_j^{A''}(s) + \omega^2 \phi_j^2 L_j^A(s) = 0,$$

that can be written in the following form

$$\tan(\alpha_j s) = -\frac{M_{2j} e^{\beta_j s} + M_{4j} e^{-\beta_j s}}{M_{1j} e^{\beta_j s} + M_{3j} e^{-\beta_j s}}, \quad (4.13)$$

where

$$\begin{aligned} M_{1j} &= (1 - \nu) \phi_j \left[(\alpha_j^2 + \beta_j^2 + k^2 + 2k\beta_j) - \omega^2 \phi_j^2 \right] B_j + 2(1 - \nu) \phi_j (k + \beta_j) \alpha_j A_j, \\ M_{2j} &= (1 - \nu) \phi_j \left[(\alpha_j^2 - \beta_j^2 - k^2 - 2k\beta_j) - \omega^2 \phi_j^2 \right] A_j - 2(1 - \nu) \phi_j (k + \beta_j) \alpha_j B_j, \\ M_{3j} &= (1 - \nu) \phi_j \left[(\alpha_j^2 - \beta_j^2 - k^2 + 2k\beta_j) - \omega^2 \phi_j^2 \right] D_j + 2(1 - \nu) \phi_j (k - \beta_j) \alpha_j C_j, \\ M_{4j} &= (1 - \nu) \phi_j \left[(\alpha_j^2 - \beta_j^2 - k^2 + 2k\beta_j) - \omega^2 \phi_j^2 \right] C_j - 2(1 - \nu) \phi_j (k - \beta_j) \alpha_j D_j. \end{aligned}$$

In section 5 we will numerically solve this equation in order to obtain the value of s (the position of the "neutral plane") as a function of the ratio E_0/E_h .

4.2 Problem B

We now require

$$\sigma_z^B(r, 0) = 0, \quad \sigma_z^B(r, h) = 0, \quad \tau_{rz}^B(r, 0) = 0, \quad \tau_{rz}^B(r, h) = 0, \quad (4.14)$$

$$w^B(b, z) = 0, \quad u^B(b, z) = -u^A(b, z). \quad (4.15)$$

By accounting for expressions (4.1) and (4.2), conditions (4.14) imply

$$\alpha''(z)\Big|_{z=0} = 0 \quad \text{and} \quad \alpha''(z)\Big|_{z=h} = 0. \quad (4.16)$$

The general expression for a function $\alpha(z)$ satisfying these conditions is

$$\alpha(z) = (z-h)^3[a_0 + a_1z + a_2z^2 + z^3A(z)],$$

for any choice of the coefficients a_0, a_1, a_2 and of the function $A(z)$.

Let us write the Plevako function $L(r, z)$ for this problem as

$$L^B(r, z) = L^{0B}(r, z) + L^{1B}(r, z), \quad (4.17)$$

where we have denoted with $L^{0B}(r, z)$ a functional contribution of the kind (3.17). On the other hand, by using (4.1), equation (3.12) becomes

$$F_j^B(z) = -2 \frac{(2 + \omega^2) \alpha''(z) - 4k \alpha'(z) - (4k^2\omega^2 + \phi_j^2) \alpha(z)}{\phi_j b J_1(\phi_j b)},$$

and

$$L_j^{1B}(z) = \frac{e^{kz} F_j^B(z) R_j(z)}{k \omega (\alpha_j^2 + \beta_j^2) \phi_j^2 b J_1(\phi_j b)}. \quad (4.18)$$

For any choice of the function $\alpha(z)$, $R_j(z)$ is given by (3.15) and, then, the coefficients A_j, B_j, C_j, D_j are obtained by conditions (4.14). Finally, the requirement $u^B(b, z) = -u^A(b, z)$ is used to identify the function $\alpha(z)$.

Due to the complexity of the expressions (3.19) and (4.7), we are not able to explicitly determine $\alpha(z)$. Hence, we follow an *inverse method* trying to find a function $\alpha(z)$ able to match the requirement (4.15) on the radial displacement with a very good approximation.

To this purpose, we *choose* the following form of $\alpha(z)$, satisfying condition (4.16):

$$\alpha(z) = (z-h)^3(a_0 + a_1z + a_2z^2 + a_3z^3 + a_4z^3 e^{kz}), \quad (4.19)$$

where $a_2 = 3(ha_1 - a_0)/h^2$. The four coefficients a_0, a_1, a_3, a_4 are arbitrary and so equation (4.19) generates *four classes of exact solutions*. We also set

$$\beta(z) = \sum_{j=2}^8 b_j z^j + \sum_{j=0}^8 \bar{b}_j z^j e^{kz}, \quad (4.20)$$

where the coefficients b_j, \bar{b}_j are obtained from a_0, a_1, a_3, a_4 by imposing equation (4.1) for $\alpha(z)$ (see Appendix 1).

By computing the integral (3.15) with the choice (4.19), one realizes that the function $L^{1B}(r, z)$ can be written as

$$L^{1B}(r, z) = \beta(z) + \sum_{j=0}^6 (G_j(r) + V_j(r) e^{kz}) z^j, \quad (4.21)$$

up to a term which can be reabsorbed in the definition of $L^{0B}(r, z)$. We have denoted with $G_j(r)$ and $V_j(r)$ suitable functions which can be now determined directly by substituting

(4.17) in (3.4); since the term $L^{0B}(r, z)$ already verifies (3.4), this procedure leads to the following systems of ordinary differential equations

$$\begin{aligned}
& \nabla_r^4 G_6(r) - 4k^2\omega^2 \nabla_r^2 G_6(r) + 4k^2\omega^2 \bar{a}_6 = 0, \\
& \nabla_r^4 G_5(r) - 4k^2\omega^2 \nabla_r^2 G_5(r) - 24k \nabla_r^2 G_6(r) + 4k^2\omega^2 \bar{a}_5 + 24k \bar{a}_6 = 0, \\
& \nabla_r^4 G_4(r) - 4k^2\omega^2 \nabla_r^2 G_4(r) - 20k \nabla_r^2 G_5(r) + 60 \nabla_r^2 G_6(r) \\
& \quad + 120k^2 G_6(r) + 4k^2\omega^2 \bar{a}_4 + 20k \bar{a}_5 - 30(\omega^2 + 2) \bar{a}_6 = 0, \\
& \nabla_r^4 G_3(r) - 4k^2\omega^2 \nabla_r^2 G_3(r) - 16k \nabla_r^2 G_4(r) + 40 \nabla_r^2 G_5(r) \\
& \quad + 80k^2 G_5(r) - 480k G_6(r) + 4k^2\omega^2 \bar{a}_3 + 16k \bar{a}_4 - 20(\omega^2 + 2) \bar{a}_5 = 0, \\
& \nabla_r^4 G_2(r) - 4k^2\omega^2 \nabla_r^2 G_2(r) - 12k \nabla_r^2 G_3(r) + 24 \nabla_r^2 G_4(r) + 48k^2 G_4 \\
& \quad (r) - 240k G_5(r) + 360 G_6(r) + 4k^2\omega^2 \bar{a}_2 + 12k \bar{a}_3 - 12(\omega^2 + 2) \bar{a}_4 = 0, \\
& \nabla_r^4 G_1(r) - 4k^2\omega^2 \nabla_r^2 G_1(r) - 8k \nabla_r^2 G_2(r) + 12 \nabla_r^2 G_3(r) \\
& \quad + 24k^2 G_3(r) - 96k G_4(r) + 120 G_5(r) + 4k^2\omega^2 \bar{a}_1 + 8k \bar{a}_2 - 6(\omega^2 + 2) \bar{a}_3 = 0, \\
& \nabla_r^4 G_0(r) - 4k^2\omega^2 \nabla_r^2 G_0(r) - 4k \nabla_r^2 G_1(r) + 4 \nabla_r^2 G_2(r) \\
& \quad + 8k^2 G_2(r) - 24k G_3(r) + 24 G_4(r) + 4k^2\omega^2 \bar{a}_0 + 4k \bar{a}_1 - 2(\omega^2 + 2) \bar{a}_2 = 0,
\end{aligned} \tag{4.22}$$

$$\begin{aligned}
& \nabla_r^4 V_6(r) - 2(2\omega^2 + 1) k^2 \nabla_r^2 V_6(r) + [\bar{b}_6 + V_6(r)] k^4 = 0, \\
& \nabla_r^4 V_5(r) - 2(2\omega^2 + 1) k^2 \nabla_r^2 V_5(r) + [\bar{b}_5 + V_5(r)] k^4 = 0, \\
& \nabla_r^4 V_4(r) - 2(2\omega^2 + 1) k^2 \nabla_r^2 V_4(r) + 60 \nabla_r^2 V_6(r) \\
& \quad + [\bar{b}_4 + V_4(r)] k^4 - 60 [\bar{b}_6 + V_6(r)] k^2 = 0, \\
& \nabla_r^4 V_3(r) - 2(2\omega^2 + 1) k^2 \nabla_r^2 V_3(r) + 40 \nabla_r^2 V_5(r) \\
& \quad + [\bar{b}_3 + V_3(r)] k^4 - 40 [\bar{b}_5 + V_5(r)] k^2 = 0, \\
& \nabla_r^4 V_2(r) - 2(2\omega^2 + 1) k^2 \nabla_r^2 V_2(r) + 24 \nabla_r^2 V_4(r) \\
& \quad + [\bar{b}_2 + V_2(r)] k^4 - 24 [\bar{b}_4 + V_4(r)] k^2 + 360 [\bar{b}_6 + V_6(r)] = 0, \\
& \nabla_r^4 V_1(r) - 2(2\omega^2 + 1) k^2 \nabla_r^2 V_1(r) + 12 \nabla_r^2 V_3(r) \\
& \quad + [\bar{b}_1 + V_1(r)] k^4 - 12 [\bar{b}_3 + V_3(r)] k^2 + 120 [\bar{b}_5 + V_5(r)] = 0, \\
& \nabla_r^4 V_0(r) - 2(2\omega^2 + 1) k^2 \nabla_r^2 V_0(r) + 4 \nabla_r^2 V_2(r) \\
& \quad + [\bar{b}_0 + V_0(r)] k^4 - 4 [\bar{b}_2 + V_2(r)] k^2 + 24 [\bar{b}_4 + V_4(r)] = 0,
\end{aligned} \tag{4.23}$$

where we have introduced the coefficients \bar{a}_j , for $j = 0, \dots, 6$ satisfying the following position

$$(z - h)^3 (a_0 + a_1 z + a_2 z^2 + a_3 z^3) = \sum_{j=0}^6 \bar{a}_j z^j.$$

The solutions of these systems, regular in $r = 0$, are

$$\begin{aligned}
G_6(r) &= g_{6,0} + g_{6,1} r^2, & G_5(r) &= g_{5,0} + g_{5,1} r^2, \\
G_4(r) &= g_{4,0} + g_{4,1} r^2 + g_{4,2} r^4 + \bar{g}_{4,0} I_0(2k\omega r), \\
G_3(r) &= g_{3,0} + g_{3,1} r^2 + g_{3,2} r^4 + \bar{g}_{3,0} I_0(2k\omega r) + \bar{g}_{3,1} r I_1(2k\omega r), \\
G_2(r) &= g_{2,0} + g_{2,1} r^2 + g_{2,2} r^4 + g_{2,3} r^6 + \bar{g}_{2,0} I_0(2k\omega r) + \bar{g}_{2,1} r I_1(2k\omega r) \\
& \quad + \bar{g}_{2,2} r^2 I_2(2k\omega r), \\
G_1(r) &= g_{1,0} + g_{1,1} r^2 + g_{1,2} r^4 + g_{1,3} r^6 + \bar{g}_{1,0} I_0(2k\omega r) + \bar{g}_{1,1} r I_1(2k\omega r) \\
& \quad + \bar{g}_{1,2} r^2 I_2(2k\omega r) + \bar{g}_{1,3} r^3 I_3(2k\omega r), \\
G_0(r) &= g_{0,0} + g_{0,1} r^2 + g_{0,2} r^4 + g_{0,3} r^6 + g_{0,4} r^8 + \bar{g}_{0,0} I_0(2k\omega r) \\
& \quad + \bar{g}_{0,1} r I_1(2k\omega r) + \bar{g}_{0,2} r^2 I_2(2k\omega r) + \bar{g}_{0,3} r^3 I_3(2k\omega r) + \bar{g}_{0,4} r^4 I_4(2k\omega r),
\end{aligned} \tag{4.24}$$

$$\begin{aligned}
V_6(r) &= v_{6,0} I_0(k\eta r) + \bar{v}_{6,0} I_0(k\psi r) - \bar{b}_6, \\
V_5(r) &= v_{5,0} I_0(k\eta r) + \bar{v}_{5,0} I_0(k\psi r) - \bar{b}_5, \\
V_4(r) &= v_{4,0} I_0(k\eta r) + \bar{v}_{4,0} I_0(k\psi r) + v_{4,1r} I_1(k\eta r) + \bar{v}_{4,1r} I_1(k\psi r) - \bar{b}_4, \\
V_3(r) &= \bar{v}_{3,0} I_0(k\psi r) + v_{3,0} I_0(k\eta r) + v_{3,1r} I_1(k\eta r) + \bar{v}_{3,1r} I_1(k\psi r) - \bar{b}_3, \\
V_2(r) &= v_{2,0} I_0(k\eta r) + \bar{v}_{2,0} I_0(k\psi r) + v_{2,1r} I_1(k\eta r) + \bar{v}_{2,1r} I_1(k\psi r) \\
&\quad + v_{2,2r^2} I_2(k\eta r) + \bar{v}_{2,2r^2} I_2(k\psi r) - \bar{b}_2, \\
V_1(r) &= v_{1,0} I_0(k\eta r) + \bar{v}_{1,0} I_0(k\psi r) + v_{1,1r} I_1(k\eta r) + \bar{v}_{1,1r} I_1(k\psi r) \\
&\quad + v_{1,2r^2} I_2(k\eta r) + \bar{v}_{1,2r^2} I_2(k\psi r) - \bar{b}_1, \\
V_0(r) &= v_{0,0} I_0(k\eta r) + \bar{v}_{0,0} I_0(k\psi r) + v_{0,1r} I_1(k\eta r) + \bar{v}_{0,1r} I_1(k\psi r) \\
&\quad + v_{0,2r^2} I_2(k\eta r) + \bar{v}_{0,2r^2} I_2(k\psi r) + v_{0,3r^3} I_3(k\eta r) + \bar{v}_{0,3r^3} I_3(k\psi r) - \bar{b}_0,
\end{aligned} \tag{4.25}$$

where $\eta = \sqrt{\omega^2 + 1} - \omega$, $\psi = \sqrt{\omega^2 + 1} + \omega$, and $I_i(x)$ denotes the i -th modified Bessel functions of the first kind. The coefficients g_{ji} , \bar{g}_{ji} , v_{ji} , and \bar{v}_{ji} are determined by solving the algebraic system which arises with their substitution in (3.4) and by accounting for the conditions $L^1(b, z) = \beta(z)$ and $\nabla_r^2 L^1(r, z)|_{r=b} = \alpha(z)$. These coefficients, given in Appendix 2, depend on the constitutive and geometrical properties of the body.

The Plevako function so obtained gives rise to the following stress components

$$\begin{aligned}
\sigma_z(r, z) &= \sigma_z^0(r, z) + c_6(z)r^4 + c_7(z)r^2 + c_8(z) \\
&\quad + [c_1(z)r^4 + c_2(z)r^2 + c_3(z)] I_0(2k\omega r) + [c_4(z)r^3 + c_5(z)r] I_1(2k\omega r) \\
&\quad + [\bar{c}_1(z)r^2 + \bar{c}_2(z)] I_0(k\eta r) + [\bar{c}_3(z)r^2 + \bar{c}_4(z)] I_0(k\psi r) \\
&\quad + [\bar{c}_6(z)r^3 + \bar{c}_5(z)r] I_1(k\eta r) + [\bar{c}_8(z)r^3 + \bar{c}_7(z)r] I_1(k\psi r), \\
\tau_{rz}(r, z) &= \tau_{rz}^0(r, z) + d_5(z)r^3 + d_6(z)r \\
&\quad + [d_1(z)r^3 + d_2(z)r] I_0(2k\omega r) + [d_3(z)r^2 + d_4(z)] I_1(2k\omega r) \\
&\quad + [\bar{d}_1(z)r^3 + \bar{d}_2(z)r] I_0(k\eta r) + [\bar{d}_4(z)r^2 + \bar{d}_3(z)] I_1(k\eta r) \\
&\quad + [\bar{d}_5(z)r^3 + \bar{d}_6(z)r] I_0(k\psi r) + [\bar{d}_8(z)r^2 + \bar{d}_7(z)] I_1(k\psi r),
\end{aligned} \tag{4.26}$$

where the functions $c_j(z)$, $d_j(z)$, $\bar{c}_i(z)$, and $\bar{d}_i(z)$ can be obtained by (3.2), (4.17), (4.21), (4.24), and (4.25).

In order to impose the boundary conditions (4.14) for $L^B(r, z)$, we compute the expressions (4.26) on the ends; the quantities $\sigma_z^0(r, 0)$, $\sigma_z^0(r, h)$, $\tau_{rz}^0(r, 0)$, and $\tau_{rz}^0(r, h)$, defined by (3.25), are written in terms of the coefficients A_j, B_j, C_j, D_j of $L^{0B}(r, z)$. To this end, we first write $\sigma_z(r, 0)$ and $\sigma_z(r, h)$ as Bessel $J_0(\phi_j r)$ expansions and $\tau_{rz}(r, 0)$ and $\tau_{rz}(r, h)$ as Dini $J_1(\phi_j r)$ expansions and, then, we solve the corresponding algebraic system obtained from their substitution in (4.14).²

This procedure leads to an algebraic system for A_j, B_j, C_j, D_j which generates four class of exact elastic *homogeneous* solutions (Lur'e 1964), for every choice of the coefficients a_0, a_1, a_3, a_4 .

The solution of the problem B can be so written as

$$L^B(r, z) = L^B(r, z; a_0, a_1, a_3, a_4),$$

²In this calculation one has to perform some integrals involving products of Bessel functions; they can be obtained by suitably differentiating, with respect to x and/or y , the expression $\int_0^b J_0(x\rho) I_0(y\rho) \rho d\rho = [x J_1(xb) I_0(yb) + y J_0(xb) I_1(yb)] b/(x^2 + y^2)$ and then substituting $x = \phi_j$ and $y = 2k\omega$.

where we have emphasised the functional dependence on the coefficients a_0, a_1, a_3, a_4 .

By using equation (3.19), we compute the resulting radial field:

$$u^B(b, z) = a_0 u^{(0)}(b, z) + a_1 u^{(1)}(b, z) + a_3 u^{(3)}(b, z) + a_4 u^{(4)}(b, z), \quad (4.27)$$

where $u^{(i)}(b, z)$ (with $i = 0, 1, 3, 4$) denotes the contribution to $u^B(b, z)$ given by the a_i -term of $\alpha(z)$.

Furthermore, we remark that, by using equations (4.2) and (4.19), the superposition principle allows us to write the explicit form of the stress on the mantle as:

$$\sigma_{\vartheta}^B(b, z) = \omega^2 \alpha''(z) - \sigma_{\vartheta}^A(b, z), \quad \sigma_z^B(b, z) = \omega^2 \alpha''(z), \quad \sigma_r^B(b, z) = \alpha''(z) - \sigma_r^A(b, z).$$

In the next section we provide an example where the coefficients a_0, a_1, a_3, a_4 generate a good approximation of the displacement field $u^B(b, z)$ opposite to the displacement (4.7). Hence, by further superposing this solution of problem B to that of problem A, we will be able to solve the global problem formulated in section 2.

5 Numerical example

The numerical example here concerned has the purpose of highlighting the peculiarity of the analytic solution obtained. Hence, we choose a thick plate-like body, having radius $b = 45$ mm and thickness $h = 15$ mm, with a quite severe Young's modulus gradation, as $E(z)$ varies from $E_h = 45$ MPa to $E_0 = 4500$ MPa, so that $k \approx 0.1535$ mm⁻¹. The Poisson ratio is uniformly $\nu = 0.3$.

The finite element model has been developed within the code ABAQUS (Dassault Systèmes, 2006). The Young's modulus variation through the thickness has been assigned by coding it into a user subroutine, so that we do not need any special finite element, as instead employed by other investigators (e.g., Kim and Paulino 2002).

The plate is loaded on the upper face by a distributed load shaped as the first term of the Bessel expansion (4.6):³

$$p(r) = J_0(\phi_1 r) \quad [\text{MPa}]. \quad (5.1)$$

Of course, different loading conditions can be obtained by superposing a suitable number of terms of the Bessel expansion.

The finest mesh employed consists of 720×240 axisymmetric 4-noded elements with full integration (four integration points each). We have implemented several models, increasing the degrees of freedom to be sure to best represent the stresses about the mantle, which is a region where, in fact, the finite element description turned out to be too much inaccurate.

³The load (5.1) has been applied to the finite element model by implementing it into a user subroutine in the following polynomial form, well fitting $J_0(\phi_1 r)$:

$$p(r) = [1 - (\phi_1 r)^2/4 + (\phi_1 r)^4/64 - (\phi_1 r)^6/2304 + (\phi_1 r)^8/147456] \quad [\text{MPa}].$$

In order to validate the solution method and get an insight into the convergence of the series involved in the analytic solutions, it is important to compare separately the solutions of the two problems A and B.

5.1 Numerical results - solution A

By using the loading condition (5.1), the solution of the problem A is obtained in closed form. In particular, equation (4.13) gives the position of the neutral plane: $s \cong 0.2h$, where $u^A(r, s) = 0$ and, by (4.12), $\sigma_r^A(b, s) = -\sigma_\vartheta^A(b, s) = 0$. In figure 2 we have plotted s/h as a function of the ratio E_0/E_h .

We remark that in the FEM approach of the problem A we need to assign the radial displacement on the mantle provided by (4.7).⁴

The analytic and the FEM solutions are in excellent agreement. In terms of displacement, they provide (within a four digits precision) exactly the same results; for instance, $w^A(0, 0) = 0.02289b$, while the maximum value occurs at $z_0 = 0.181h$ and reads $w^A(0, z_0) = 0.023b$.

The behaviour in terms of stresses is given in figure 3, which shows the radial and shear stresses through the plate thickness, in the centre and on the mantle. The comparisons give very satisfactory results. Figure 4 gives a further insight on the stress behaviour by showing the radial and circumferential stress variation along the ends. It is clearly recognised that $\sigma_r^A(0, z) = \sigma_\vartheta^A(0, z)$ and $\sigma_r^A(b, z) = -\sigma_\vartheta^A(b, z)$.

5.2 Numerical results - solution B

The analytic solution of subsection 4.2 requires the calculation of the coefficients a_0, a_1, a_3, a_4 of (4.27) in order to assign the required radial displacement on the mantle.

We use a least square technique to find the coefficients a_0, a_1, a_3, a_4 best fitting the function $u^A(b, z)$; the coefficients of (4.27) for the displacement $u^B(b, z)$ are:

$$a_0 = 0.4613 \cdot 10^{-1}, \quad a_1 = 0.8980 \cdot 10^{-2}, \quad a_3 = 0.5810 \cdot 10^{-4}, \quad a_4 = -0.9662 \cdot 10^{-3}. \quad (5.3)$$

As shown by the first two curves in figure 5, the radial displacement $u^A(b, z)$ (5.2) and the displacement generated by the procedure of solution described in subsection 4.2 are in a very good agreement.

We remark that the FEM solution is obtained by applying $u^B(b, z) = -u^A(b, z)$ as given by (5.2), instead of its approximation employed in the analytic procedure. The transversal displacement is $w^B(0, 0) = -0.0130974b$ whereas the FEM results provides $w_{\text{FEM}}^B(0, 0) =$

⁴To this purpose, we have implemented into a user subroutine the following numerical evaluation of the displacement provided by equation (4.7):

$$u^A(b, z) = h \left[e^{4.7885z/h} \left(1.3221 \times 10^{-5} \sin(qz/h) + 8.7208 \times 10^{-6} \cos(qz/h) \right) + e^{-0.18352z/h} \left(5.6634 \times 10^{-2} \sin(qz/h) - 5.4937 \times 10^{-3} \cos(qz/h) \right) \right] \quad (5.2)$$

where $q \cong 0.48604$.

$-0.01302b$. The maximum transversal displacement predicted by the analytic solution is $w^B(0, z_0) = -0.0131501b$, with $z_0 \approx 0.181h$, while $w_{\text{FEM}}^B(0, z_0) = -0.01307b$.

In figure 6 we have reported the radial and circumferential stresses on the plate ends in terms of the normalised radial coordinate. From the black and red plots on this figure it is evicted that the results are in excellent agreement within the region $r \in [0, \approx 0.85b]$, while there is a large discrepancy approaching the mantle.

Figure 7 shows that the FEM approach is quite inaccurate in predicting the stresses about the mantle. In fact, *as quite satisfactorily predicted by the analytic solution, both $\sigma_z(b, z)$ and $\tau_{rz}(b, z)$ should be zero in the mantle corners ($z = 0$ and $z = h$)*, while, for $z \rightarrow 0$, the FEM analysis predicts that they both reach a conspicuous maximum value, even larger than the maximum radial stress on the mantle. This problem is due to the simultaneous presence of high stress gradients, corners, and nodes having all the degrees of freedom assigned. We notice that this problem cannot be solved by further refining the mesh, or by choosing other standard or hybrid elements: for each formulation, we tried both 4-noded and 8-noded elements, with either full or reduced integration, always obtaining very similar results. Elements with incompatible modes mitigate the corner problem, but they do not solve it.

The discrepancy between the analytical and FEM solutions is instead less pronounced if the FEM solution is obtained by applying at the mantle the same displacement as that employed in the analytical solution, instead of $-u^A(b, z)$. However, since we have no simple explicit analytical expression for the displacement $u^B(b, z)$ given by (4.27), we can apply to the FEM model a polynomial best fitting it. Figures 6 and 7 report the results corresponding to the choice of a 6th-order polynomial for representing $u^B(b, z)$, as plotted in figure 5.⁵ The solution is mostly improved in the upper face, while it is still quite far from the analytic solution in the bottom face, where, by the way, as shown in the detail of figure 5, the chosen 6th-order polynomial is less precise in fitting the radial displacement $u^B(b, z)$ given by (4.27).

The results in terms of stresses show a very large sensitivity to changing the applied displacement by a small perturbation, which is for instance the case of the difference between $-u^A(b, z)$ and its approximation (4.27) with the coefficients given in equation (5.3). This suggests that simpler models than that here developed, where only average boundary conditions can be imposed at the mantle, may provide stresses about the mantle very different from that actual ones.

In any case, within the conventional FEM formulation employed, the element in the corner ($r = b, z = 0$) cannot satisfy both the field and the boundary equations.

Note that in Problem A we have shown, in the previous subsection 5.1, that the numerical

⁵The polynomial, implemented within a 15 digits precision, fits $u^B(b, z)$ with a determination coefficient $R^2 = 0.999901$ and reads

$$u_{\text{pol}}^B(b, z) \approx -3.2071(z/h)^6 + 8.14320(z/h)^5 - 6.6591(z/h)^4 \\ + 1.4245(z/h)^3 + 0.42051(z/h)^2 - 0.243022z/h - 0.073364$$

solution is quite accurate, also at the mantle, in spite of the similarity of problems A and B in terms of boundary conditions. This might be due to the presence, in Problem A, of the load $p(r)$, which is strictly connected to the radial displacement at the mantle $u^A(b, z)$, the latter being a result of the analysis. This suggests that the *combined* boundary conditions consisting of $\sigma_z^A(r, 0) = -p(r)$ and $u(b, z) = u^A(b, z)$ leads to a Levinson type of solution which is smooth enough to be described by the FEM. Instead, in Problem B, the presence of the sole loading condition $u^B(b, z) = -u^A(b, z)$ leads to a solution (see, e.g., figure 6), whose associated displacement field turns out to be difficult to be modelled via FEM. It is important to notice that this stress behaviour at the mantle, in Problem B, corresponds to the existence of a *non-planar neutral surface*.

Finally, let us notice that the issues above are not peculiar of FGM materials only, as one has to face with them also in the homogeneous case.

5.3 Numerical results - final solution

The complete solution is obtained by superposition of the solutions A and B. We note that the non-monotonic behaviour of $w(0, z)$ implies a change in sign of the strain $\varepsilon_z(0, z)$ and $w(0, z)$ has a variation of about 10% between its maximum and minimum values; such a variation is large enough in order to establish the invalidity for the present case of the assumption, standard for plates, of constant through-the-thickness deflection (Reddy and Cheng 2001).

Figure 8 shows, on the deformed shape, the contour of the shear stress, restricted to the region $r \in [0, 0.8b]$, where the results of the analytical and finite element solutions are almost coincident.

Let us now highlight the peculiarity of the stress behaviour on the mantle. To this purpose, we exploit the *closed form* expressions (4.2) for the stress components:

$$\sigma_r(b, z) = \alpha''(z), \quad \sigma_\vartheta(b, z) = \sigma_z(b, z) = \omega^2 \alpha''(z),$$

where $\alpha''(z)$ is obtained by equation (4.19) with the coefficients a_0, a_1, a_3, a_4 given by (5.3). While the usual classical plate models assume that σ_z vanishes everywhere, we observe that the solution of problem A states that $\sigma_z^A(r, z)$ is non-zero in the internal points whereas it is null on the mantle (see equation (4.11)). Hence, in the global problem, the function σ_z on the mantle turns out to coincide with $\sigma_z^B(b, z)$ and $\sigma_\vartheta(b, z) = \sigma_z(b, z)$.

In figure 9 we have plotted the radial and shear stresses along various radial sections. Their highly oscillatory behaviour about the mantle rapidly disappears moving towards the centre (Sburlati 2009). The radial stress at the centre is the only curve made non-dimensional by dividing it by the Young's modulus gradation (3.3); it is interesting that such a normalisation leads to an almost perfectly linear curve.

We remark that the radial stress is such that the neutral surface is non-planar, due to the edge effects on the mantle.

Effect of a graded Poisson's ratio We wish now to investigate on the assumption of uniform Poisson's ratio introduced in the analytic model. To this purpose, we have run FEM

analyses similar to those exploited so far, with the exception that we assume for the Poisson ratio an exponential variation analogous to that chosen for the Young modulus, given by equations (3.3):

$$\nu(z) = \nu_0 e^{2k_\nu z}, \quad k_\nu = \frac{1}{2h} \ln \left(\frac{\nu_h}{\nu_0} \right),$$

where $\nu(0) = \nu_0$ and $\nu(h) = \nu_h$. We have set a quite extreme variation of Poisson's ratio: $\nu_0 = 0.01$ (where $E_0 = 4500$ MPa) and $\nu_h = 0.499$ (where $E_h = 45$ MPa), according to the fact that, often, the softer the material the higher the Poisson ratio. Also, we have run other two reference analyses with spatially uniform ν having values of 0. and 0.499, respectively.

The results are given in terms of the most significant variables at the centre, where the finite element results are very accurate. From figure 10 one evicts that the change in the deflection $w(0, z)$ may be quite relevant, even though the maximum deflection in the case of graded Poisson's ratio is larger of only 2.8% with respect to the analysis where the Poisson ratio is uniform and equal to 0.3. As shown in figure 11, the qualitative match between different cases is better if evaluated in terms of $\sigma_r(0, z)$, albeit the maximum stress of the graded case differ of about 26% with respect to the case $\nu=0.3$. Also, it turned out that, in terms of stresses, the graded case is very similar to that of $\nu=0$, uniformly.

6 Concluding remarks

We have determined some exact 3D elastic solutions for an axisymmetric functionally graded cylinder subject to mixed boundary conditions. By assuming inhomogeneity governed by exponential gradation along the plate thickness, we have studied the case of a plate-like body perfectly clamped on the mantle and subject to a transversal distributed load on the upper face. The major effort has been devoted to assign the boundary conditions *pointwise*. The analytic solution, obtained in terms of Bessel expansions, is numerically robust since the solution is obtained as the sum of two parts: one given in closed form and the other written in a standard way, for which convergence properties are known.

The method of solution allowed us to highlight the inhomogeneity effects, to show the non-planarity of the neutral surface due to the localized effects on the edges, and to obtain the stress behaviour on the mantle in a closed form. The comparisons with a FEM approach have been very satisfactory in internal points and showed the relevant difficulties in representing the solution near the mantle because of the large sensitivity of the solution within the mantle region to the boundary conditions and because of the inability of the conventional finite elements employed to satisfy all the equilibrium conditions in the corner region.

Moreover, the investigation with FEM on the effects of a graded Poisson's ratio, in conjunction with the Young's modulus gradation, quantified the limits of the usual assumptions introduced in the literature to obtain analytic solutions.

Finally, we observe that the method of solution may be adopted to account different boundary conditions and to describe the elastic response of a FGM coating on a substrate (see, e.g., Kashtalyan and Menshykova 2008).

Acknowledgements

Work financed by the Italian Ministry of Education, University, and Research (MIUR). The first author acknowledges the support of Prin2007 Project No.2007YZ3B24: "Multiscale problems with complex interactions in Structural Engineering". The Authors wish to thank Professor Paul Wawryznek for useful discussions.

Appendix 1

The coefficients of (4.20) are

$$\begin{aligned}
b_2 &= \frac{1}{4k^6}(\omega^2 + 1) (45 \bar{a}_6 + 15k \bar{a}_5 + 6k^2 \bar{a}_4 + 3k^3 \bar{a}_3 + 2k^4 \bar{a}_2 + 2k^5 \bar{a}_1) + \frac{1}{2} \omega^2 \bar{a}_0, \\
b_3 &= \frac{1}{6k^5}(\omega^2 + 1) (45 \bar{a}_6 + 15k \bar{a}_5 + 6k^2 \bar{a}_4 + 3k^3 \bar{a}_3 + 2k^4 \bar{a}_2) + \frac{1}{6} \omega^2 \bar{a}_1, \\
b_4 &= \frac{1}{4k^4}(\omega^2 + 1) (15 \bar{a}_6 + 5k \bar{a}_5 + 2k^2 \bar{a}_4 + k^3 \bar{a}_3) + \frac{1}{12} \omega^2 \bar{a}_2, \\
b_5 &= \frac{1}{10k^3}(\omega^2 + 1) (15 \bar{a}_6 + 5k \bar{a}_5 + 2k^2 \bar{a}_4) + \frac{1}{20} \omega^2 \bar{a}_3, \\
b_6 &= \frac{1}{6k^2}(\omega^2 + 1) (3 \bar{a}_6 + k \bar{a}_5) + \frac{1}{30} \omega^2 \bar{a}_4, \quad b_7 = \frac{1}{7k}(\omega^2 + 1) \bar{a}_6 + \frac{1}{42} \omega^2 \bar{a}_5, \quad b_8 = \frac{1}{56} \omega^2 \bar{a}_6, \\
\bar{b}_0 &= \frac{24}{k^8} (h^3 k^3 \omega^2 + 21 h^2 k^2 \omega^2 + 90 h k \omega^2 + 6 h^2 k^2 + 270 \omega^2 + 60) a_4, \\
\bar{b}_1 &= -\frac{6}{k^7} (5 h^3 k^3 \omega^2 + 48 h^2 k^2 \omega^2 + 420 h k \omega^2 + 2 h^3 k^3 + 120 h k + 720 \omega^2) a_4, \\
\bar{b}_2 &= \frac{6}{k^6} (h^3 k^3 \omega^2 + 30 h^2 k^2 \omega^2 + 120 h k \omega^2 + 12 h^2 k^2 + 420 \omega^2 + 120) a_4, \\
\bar{b}_3 &= -\frac{1}{k^5} (3 h^3 k^3 \omega^2 + 24 h^2 k^2 \omega^2 + 300 h k \omega^2 + 2 h^3 k^3 + 120 h k + 480 \omega^2) a_4, \\
\bar{b}_4 &= \frac{3}{k^4} (3 h^2 k^2 \omega^2 + 10 h k \omega^2 + 2 h^2 k^2 + 50 \omega^2 + 20) a_4, \\
\bar{b}_5 &= -\frac{3}{k^3} (3 h k \omega^2 + 2 h k + 4 \omega^2) a_4, \quad \bar{b}_6 = \frac{1}{k^2} (3 \omega^2 + 2) a_4.
\end{aligned}$$

Appendix 2

By setting $\sqrt{\omega^2 + 1} = \chi$, we write:

$$\begin{aligned}
g_{6,0} &= -\frac{b^2}{4} \bar{a}_6, \quad g_{5,0} = -\frac{b^2}{4} \bar{a}_5, \quad g_{4,0} = -\frac{b^2}{4} \bar{a}_4 + \frac{15 A_{4,0}}{32 k^4 \omega^6} \bar{a}_6, \\
g_{3,0} &= -\frac{b^2}{4} \bar{a}_3 + \frac{5 A_{4,0}}{16 k^4 \omega^6} \bar{a}_5 - \frac{15 A_{3,0}}{8 k^5 \omega^8} \bar{a}_6, \quad g_{2,0} = \frac{3 A_{4,0}}{16 k^4 \omega^6} \bar{a}_4 - \frac{15 A_{3,0}}{16 k^5 \omega^8} \bar{a}_5 - \frac{5 A_{2,0}}{32 k^6 \omega^{10}} \bar{a}_6, \\
g_{1,0} &= -\frac{b^2}{4} \bar{a}_1 + \frac{3 A_{4,0}}{32 k^4 \omega^6} \bar{a}_3 - \frac{3 A_{3,0}}{8 k^5 \omega^8} \bar{a}_4 - \frac{5 A_{2,0}}{96 k^6 \omega^{10}} \bar{a}_5 - \frac{5 A_{1,0}}{16 k^7 \omega^{12}} \bar{a}_6, \\
g_{0,0} &= -\frac{b^2}{4} \bar{a}_0 - \frac{3 A_{3,0}}{32 k^5 \omega^8} \bar{a}_3 - \frac{A_{2,0}}{96 k^6 \omega^{10}} \bar{a}_4 + \frac{5 A_{1,0}}{96 k^7 \omega^{12}} \bar{a}_5 + \frac{5 A_{0,0}}{1024 k^8 \omega^{14}} \bar{a}_6, \\
g_{6,1} &= \frac{1}{4} \bar{a}_6, \quad g_{5,1} = \frac{1}{4} \bar{a}_5, \quad g_{4,1} = \frac{1}{4} \bar{a}_4 - \frac{15 A_{4,1}}{8 k^2 \omega^4} \bar{a}_6, \\
g_{3,1} &= \frac{1}{4} \bar{a}_3 - \frac{5 A_{4,1}}{4 k^2 \omega^4} \bar{a}_5 + \frac{15 A_{3,1}}{2 k^3 \omega^6} \bar{a}_6, \quad g_{2,1} = -\frac{3 A_{4,1}}{4 k^2 \omega^4} \bar{a}_4 + \frac{15 A_{3,1}}{4 k^3 \omega^6} \bar{a}_5 + \frac{45 A_{2,1}}{32 k^4 \omega^8} \bar{a}_6,
\end{aligned}$$

$$\begin{aligned}
g_{1,1} &= \frac{1}{4} \bar{a}_1 - \frac{3 A_{4,1}}{8 k^2 \omega^4} \bar{a}_3 + \frac{3 A_{3,1}}{2 k^3 \omega^6} \bar{a}_4 + \frac{15 A_{2,1}}{32 k^4 \omega^8} \bar{a}_5 + \frac{45 A_{1,1}}{8 k^5 \omega^{10}} \bar{a}_6, \\
g_{0,1} &= \frac{1}{4} \bar{a}_0 + \frac{3 A_{3,1}}{8 k^3 \omega^6} \bar{a}_3 + \frac{3 A_{2,1}}{32 k^4 \omega^8} \bar{a}_4 + \frac{15 A_{1,1}}{8 k^5 \omega^{10}} \bar{a}_5 + \frac{A_{0,1}}{64 k^6 \omega^{12}} \bar{a}_6, \\
g_{4,2} &= \frac{15}{32 \omega^2} \bar{a}_6, \quad g_{3,2} = \frac{5}{16 \omega^2} \bar{a}_5 - \frac{15 \chi^2}{k \omega^4} \bar{a}_6, \quad g_{2,2} = \frac{3}{16 \omega^2} \bar{a}_4 - \frac{15 \chi^2}{16 k \omega^4} \bar{a}_5 - \frac{45 A_{2,2}}{32 k^2 \omega^6} \bar{a}_6, \\
g_{1,2} &= \frac{3}{32 \omega^2} \bar{a}_3 - \frac{3 \chi^2}{8 k \omega^4} \bar{a}_4 - \frac{15 A_{2,2}}{32 k^2 \omega^6} \bar{a}_5 + \frac{45 A_{1,2}}{16 k^3 \omega^8} \bar{a}_6, \\
g_{0,2} &= -\frac{3 \chi^2}{32 k \omega^4} \bar{a}_3 - \frac{3 A_{2,2}}{32 k^2 \omega^6} \bar{a}_4 + \frac{15 A_{1,2}}{32 k^3 \omega^8} \bar{a}_5 + \frac{A_{0,2}}{256 k^4 \omega^{10}} \bar{a}_6, \quad g_{2,3} = \frac{5}{32 \omega^4} \bar{a}_6, \\
g_{1,3} &= \frac{5}{96 \omega^4} \bar{a}_5 - \frac{5 \chi^2}{8 k \omega^6} \bar{a}_6, \quad g_{0,3} = \frac{1}{96 \omega^4} \bar{a}_4 - \frac{5 \chi^2}{48 k \omega^6} \bar{a}_5 - \frac{5 A_{0,3}}{64 k^2 \omega^8} \bar{a}_6, \quad g_{0,4} = \frac{5}{1024 \omega^6} \bar{a}_6,
\end{aligned}$$

where

$$\begin{aligned}
A_{4,0} &= 3 k^4 \omega^4 b^4 + 4 \chi^2 (\omega^2 - 1) (k^2 \omega^2 b^2 - 1), \quad A_{3,0} = \chi^2 (3 k^4 \omega^4 b^4 + 4 k^2 \omega^2 b^2 (\omega^2 - 2) - 4 (2 \omega^2 - 3)), \\
A_{2,0} &= 19 k^6 \omega^6 b^6 - 18 \chi^2 (9 k^4 \omega^4 b^4 + 2 k^2 \omega^2 b^2 (2 \omega^4 + 3 \omega^2 - 15) - 4 (2 \omega^4 + 5 \omega^2 - 14)), \\
A_{1,0} &= \chi^2 k^4 \omega^3 (38 \omega^2 b^6 k^2 + 27 \omega^4 - 54 \omega^2 - 270) \\
&\quad + \chi^2 (72 (\omega^2 - (3 \omega^4 - 14)) \omega^2 k^2 b^2 - 2160 + 36 \omega^2 (15 \omega^2 + 4)), \\
A_{0,0} &= 211 b^8 \omega^8 k^8 + 1/16 [-95 \omega^6 (\omega^2 + 3) k^6 b^6 - 27 \omega^4 (\omega^6 + 9 \omega^4 - 30 \omega^2 - 70) k^4 b^4 \\
&\quad + 72 \omega^2 (3 \omega^6 + 25 \omega^4 - 35 \omega^2 - 105) k^2 b^2 - 540 \omega^6 - 5292 \omega^4 + 3780 \omega^2 + 17820] \chi^2 \\
A_{4,1} &= k^2 \omega^2 b^2 + \chi^2 (\omega^2 - 1), \quad A_{3,1} = \chi^2 (k^2 \omega^2 b^2 + (\omega^2 - 2)), \\
A_{2,1} &= 3 b^4 \omega^4 k^4 - 24 k^2 b^2 \chi^2 - 8 \omega^2 (\omega^4 - 6) - 20 (\omega^4 - 3), \\
A_{1,1} &= \chi^2 (2 b^2 \omega^6 k^2 - 4 k^2 b^2 \omega^4 - 12 \omega^4 + 3 b^4 \omega^4 k^4 + 4 \omega^2 - 20 b^2 k^2 \omega^2 + 56) \\
A_{0,1} &= 675 b^4 k^4 \omega^4 \chi^2 (\omega^2 + 3) - 95 b^6 k^6 \omega^6 + 180 b^2 k^2 \omega^2 \chi^2 (\omega^6 + 9 \omega^4 - 30 \omega^2 - 70) \\
&\quad - 360 \chi^2 (3 \omega^6 + 25 \omega^4 - 35 \omega^2 - 105), \\
A_{2,2} &= k^2 \omega^2 b^2 - 6 \chi^2, \quad A_{1,2} = \chi^2 (2 k^2 \omega^2 b^2 + \omega^4 - 2 \omega^2 - 10), \\
A_{0,2} &= 135 b^4 k^4 \omega^4 - 900 b^2 \chi^2 k^2 \omega^2 (\omega^3 + 3) - 180 \chi^2 (\omega^6 + 9 \omega^4 - 30 \omega^2 - 70), \\
A_{0,3} &= \omega^2 b^2 k^2 - 5 \omega^4 - 20 \omega^2 - 15,
\end{aligned}$$

and

$$\begin{aligned}
\bar{g}_{4,0} &= \frac{15 B_{4,0}}{8 k^4 \omega^6} \bar{a}_6, \quad \bar{g}_{3,0} = \frac{5 B_{4,0}}{4 k^4 \omega^6} \bar{a}_5 + \frac{15 B_{3,0}}{2 k^5 \omega^8} \bar{a}_6, \quad \bar{g}_{2,0} = \frac{3 B_{4,0}}{4 k^4 \omega^6} \bar{a}_4 + \frac{15 B_{3,0}}{4 k^5 \omega^8} \bar{a}_5 + \frac{45 B_{2,0}}{2 k^6 \omega^{10}} \bar{a}_6, \\
\bar{g}_{1,0} &= \frac{3 B_{4,0}}{8 k^4 \omega^6} \bar{a}_3 + \frac{3 B_{3,0}}{2 k^5 \omega^8} \bar{a}_4 + \frac{15 B_{2,0}}{2 k^6 \omega^{10}} \bar{a}_5 + \frac{15 B_{1,0}}{k^7 \omega^{12}} \bar{a}_6, \\
\bar{g}_{0,0} &= \frac{3 B_{3,0}}{8 k^5 \omega^8} \bar{a}_3 + \frac{3 B_{2,0}}{2 k^6 \omega^{10}} \bar{a}_4 + \frac{5 B_{1,0}}{2 k^7 \omega^{12}} \bar{a}_5 + \frac{15 B_{0,0}}{k^8 \omega^{14}} \bar{a}_6, \quad \bar{g}_{3,1} = \frac{15 B_{4,0}}{2 k^4 \omega^7} \bar{a}_6, \\
\bar{g}_{2,1} &= \frac{15 B_{4,0}}{4 k^4 \omega^7} \bar{a}_5 + \frac{45 (4 B_{3,0} - (2 \omega^2 + 1) B_{4,0})}{8 k^5 \omega^9} \bar{a}_6, \\
\bar{g}_{1,1} &= \frac{3 B_{4,0}}{2 k^4 \omega^7} \bar{a}_4 + \frac{15 (4 B_{3,0} - (2 \omega^2 + 1) B_{4,0})}{8 k^5 \omega^9} \bar{a}_5 + \frac{45 (4 B_{2,0} - (2 \omega^2 + 1) B_{3,0} + \chi^2 B_{4,0})}{4 k^6 \omega^{11}} \bar{a}_6, \\
\bar{g}_{0,1} &= \frac{3 B_{4,0}}{8 \omega} \bar{a}_3 + \frac{3 (4 B_{3,0} - (2 \omega^2 + 1) B_{4,0})}{8 k \omega^3} \bar{a}_4 + \frac{15 (4 B_{2,0} - (2 \omega^2 + 1) B_{3,0} + \chi^2 B_{4,0})}{8 k^2 \omega^5} \bar{a}_5
\end{aligned}$$

$$\begin{aligned}
& + \frac{15(4B_{1,0} - 3(2\omega^2 + 1)B_{2,0} + 3\chi^2 B_{3,0})}{4k^3\omega^7} \bar{a}_6 + \frac{15(18\omega^4 + 23\omega^2 - 53)(1 - k^4\omega^6)b^2 B_{4,0}}{8k^5\omega^{11}(\omega^2 - 1)} \bar{a}_6 \\
& + \frac{45(2(4\omega^6 - 17\omega^2 + 46\omega^4 - 140)\omega^6 k^4 + 285 - 97\omega^4 - 9\omega^6 + 35\omega^2)B_{4,0}}{16(\omega^2 - 1)k^7\omega^{13}} \bar{a}_6, \\
\bar{g}_{2,2} &= \frac{45B_{4,0}}{4k^4\omega^8} \bar{a}_6, & \bar{g}_{1,2} &= \frac{15B_{4,0}}{4k^4\omega^8} \bar{a}_5 + \frac{45(2B_{3,0} - (2\omega^2 + 1)B_{4,0})}{4k^5\omega^{10}} \bar{a}_6, \\
\bar{g}_{0,2} &= \frac{3B_{4,0}}{4k^4\omega^8} \bar{a}_4 + \frac{15(2B_{3,0} - (2\omega^2 + 1)B_{4,0})}{8k^5\omega^{10}} \bar{a}_5 \\
& + \frac{45(16B_{2,0} - 8(2\omega^2 + 1)B_{3,0} + (2\omega^2 + 3)^2 B_{4,0})}{32k^6\omega^{12}} \bar{a}_6, & \bar{g}_{1,3} &= \frac{15B_{4,0}}{2k^4\omega^9} \bar{a}_6, \\
\bar{g}_{0,3} &= \frac{5B_{4,0}}{4k^4\omega^9} \bar{a}_5 + \frac{15(4B_{3,0} - 3(2\omega^2 + 1)B_{4,0})}{8k^5\omega^{11}} \bar{a}_6, & \bar{g}_{0,4} &= \frac{15B_{4,0}}{8k^4\omega^{10}} \bar{a}_6,
\end{aligned}$$

where

$$\begin{aligned}
B_{4,0} &= \frac{\omega^4 - 1}{I_0(2k\omega b)}, & B_{3,0} &= -\frac{k\omega b I_1(2k\omega b)}{I_0(2k\omega b)} B_{4,0} - \frac{(2\omega^2 - 3)\chi^2}{I_0(2k\omega b)}, \\
B_{2,0} &= -\frac{bk\omega I_1(2k\omega b)}{I_0(2k\omega b)} B_{3,0} + \frac{bk\omega(2\omega^2 + 3)I_1(2k\omega b)}{4I_0(2k\omega b)} B_{4,0} - \frac{1}{2}k^2\omega^2 b^2 B_{4,0} \\
& + \frac{\chi^2(2\omega^4 + 5\omega^2 - 14)}{2I_0(2k\omega b)}, \\
B_{1,0} &= -\frac{3k\omega b I_0(2k\omega b)}{I_1(2k\omega b)} B_{2,0} + \frac{3k\omega b(2\omega^2 + 3)I_1(2k\omega b)}{4I_0(2k\omega b)} B_{3,0} \\
& + \frac{k\omega b(-9\omega^2 + 4b^2k^2\omega^2 - 10)I_1(1, 2k\omega b)}{4I_0(2k\omega b)} B_{4,0} \\
& + \frac{\chi^2(b^2k^2\omega^2(6\omega^4 + 13\omega^2 - 25) - 45\omega^4 - 12\omega^2 + 180)}{4I_0(2k\omega b)}, \\
B_{0,0} &= -\frac{k\omega b I_1(2k\omega b)}{I_0(2k\omega b)} B_{1,0} + \frac{3k\omega b(2\omega^2 + 3)I_1(2k\omega b)}{4I_0(2k\omega b)} B_{2,0} \\
& + \frac{k\omega b(-9\omega^2 + 4b^2k^2\omega^2 - 10)I_1(2k\omega b)}{4I_0(2k\omega b)} B_{3,0} + \frac{\chi^2(579b^2k^2\omega^2 - 630\omega^2 - 2970)}{32I_0(2k\omega b)} \\
& - \frac{(-18\omega^4 + 48b^2k^2\omega^4 + 64b^2k^2\omega^2 - 120\omega^2 - 105)k\omega b I_1(2k\omega b)B_{4,0}}{32I_0(2k\omega b)} \\
& + \frac{\chi^2(-12\omega^8 b^2k^2 + 90\omega^6 + 20\omega^6 k^4 b^4 - 216b^2k^2\omega^6 - 79b^2k^2\omega^4 + 882\omega^4 - 20k^4 b^4 \omega^4)}{32I_0(2k\omega b)}.
\end{aligned}$$

The coefficients v_{ji}, \bar{v}_{ji} are

$$\begin{aligned}
v_{6,0} &= \frac{\bar{b}_6 k^2 \psi^2 - a_4}{4k^2 \omega \chi I_0(k\eta b)}, & \bar{v}_{6,0} &= -\frac{\bar{b}_6 k^2 \eta^2 - a_4}{4k^2 \omega \chi I_0(k\psi b)}, & v_{5,0} &= \frac{\bar{b}_5 k^2 \psi^2 + 3a_4 h}{4k^2 \omega \chi I_0(k\eta b)}, \\
v_{4,0} &= C_1 v_{4,1} + \psi C_2 \bar{v}_{4,1} + \frac{\bar{b}_4 k^2 \psi^2 - 3a_4 h^2}{4k^2 \omega \chi I_0(k\eta b)}, & v_{3,0} &= C_1 v_{3,1} + \psi C_2 \bar{v}_{3,1} + \frac{\bar{b}_3 k^2 \psi^2 + a_4 h^3}{4k^2 \omega \chi I_0(k\eta b)}, \\
v_{2,0} &= C_1 v_{2,1} + \psi C_2 \bar{v}_{2,1} + C_3 v_{2,2} + \psi C_4 \bar{v}_{2,2} + \frac{\bar{b}_2 \psi^2}{4\omega \chi I_0(k\eta b)},
\end{aligned}$$

$$\begin{aligned}
v_{1,0} &= C_1 v_{1,1} + \psi C_2 \bar{v}_{1,1} + C_3 v_{1,2} + \psi C_4 \bar{v}_{1,2} + \frac{\bar{b}_1 \psi^2}{4\omega \chi I_0(k\eta b)}, \\
v_{0,0} &= C_1 v_{0,1} + 1/\eta C_2 \bar{v}_{0,1} + C_3 v_{0,2} + 1/\eta C_4 \bar{v}_{0,2} + C_5 v_{0,3} + 1/\eta C_6 \bar{v}_{0,3} + \frac{\bar{b}_0}{4\omega \chi \eta^2 I_0(k\eta b)}, \\
v_{4,1} &= -\frac{15}{k\chi} v_{6,0}, \quad v_{3,1} = -\frac{10}{k\chi} v_{5,0}, \quad v_{2,1} = -\frac{6}{k\chi} v_{4,0} + \frac{45\omega}{k^3 \eta \chi^3} v_{6,0}, \\
v_{1,1} &= \frac{15(2\chi\eta - 3\omega^2 + 3\omega\chi - 2)}{k^3 \chi^3 \eta^2} v_{5,0} - \frac{3}{k\chi} v_{3,0}, \quad v_{0,1} = -\frac{1}{k\chi} v_{2,0} + \frac{3\omega}{k^3 \chi^3 \eta} v_{4,0} + \frac{45\omega}{k^5 \chi^5 \eta} v_{6,0}, \\
v_{2,2} &= \frac{45}{k^2 \chi^2} v_{6,0}, \quad v_{1,2} = \frac{15}{k^2 \chi^2} v_{5,0}, \quad v_{0,2} = \frac{3}{k^2 \chi^2} v_{4,0} - \frac{45\omega}{k^4 \chi^4 \eta} v_{6,0}, \quad v_{0,3} = -\frac{15}{k^3 \chi^3} v_{6,0}, \\
\text{where } C_1 &= \frac{\eta}{2k\omega\chi} - \frac{bI_1(k\eta b)}{I_0(k\eta b)}, \quad C_2 = \frac{I_0(k\psi b)}{2k\omega\chi I_0(k\eta b)}, \quad C_3 = \frac{(2\omega^2 + 1)bI_1(k\eta b)}{k\omega\chi\eta I_0(k\eta b)} - b^2 \\
C_4 &= \frac{bI_1(k\psi b)}{k\omega\chi I_0(k\eta b)}, \quad C_6 = \frac{3b(bkI_0(k\psi b) - 2\eta I_1(k\psi b))}{2k^2\omega\chi\eta I_0(k\eta b)} \\
C_5 &= \frac{(4\eta\chi^2 + 3\omega - \chi)b^2}{2k\omega\chi\eta^2} + \frac{(3 - 2\omega\chi - 6\chi^2 - \omega\chi k^2\eta^2 b^2)bI_1(k\eta b)}{k^2\omega\chi\eta^2 I_0(k\eta b)}.
\end{aligned}$$

The coefficients $\bar{v}_{i,j}$ can be obtained from the analogous coefficients $v_{i,j}$ by exchanging ψ with η and changing a sign, after having written in terms of coefficients a_i and \bar{b}_i .

References

- Chan, Y.-S., Gray, L.J., Kaplan, T., Paulino, G.H., 2004. Green's function for a two-dimensional exponentially graded elastic medium. *Proc. R. Soc. London A* 460, 1689-1706.
- Dassault Systèmes, 2006. ABAQUS User's & Theory Manuals — Release 6.6, Providence, RI (USA).
- Elishakoff, I., Gentilini, C., 2005. Three-dimensional flexure of rectangular plates made of functionally graded material. *J. Appl. Mech.-T ASME* 72, 788-791.
- Erdogan, F., 1995. Fracture mechanics of functionally graded materials. *Compos. Eng.* 5, 753-777.
- Kashtalyan, M., 2004. Three-dimensional elasticity solution for bending of functionally graded rectangular plates. *Eur. J. Mech. A-Solid*. 23, 853-864.
- Kashtalyan, M., Menshykova, M., 2008. Three-dimensional analysis of a functionally graded coating/substrate system of finite thickness. *Proc. R. Soc. London A* 366, 1821-1826.
- Kim, J.-H., Paulino, G.H., 2002. Isoparametric graded finite elements for nonhomogeneous isotropic and orthotropic materials. *J. Appl. Mech.-T ASME* 69, 502-514.
- Levinson, M., 1985. The simply supported rectangular plate: an exact, three-dimensional, linear elastic solution. *J. Elast.* 7, 283-291.
- Li, X.Y., Ding, H.J., Chen, W.Q., 2008. Elasticity solutions for a transversely isotropic functionally graded circular plate subject to an axisymmetric transverse load qr^k . *Int. J. Solids Struct.* 45, 191-210.

- Love, A.E.H., 1927. *A Treatise on the Mathematical Theory of Elasticity*, fourth ed. Cambridge University Press, Cambridge (UK).
- Lur'e, A.I., 1964. *Three-Dimensional Problems of the Theory of Elasticity*, Interscience, New York.
- Ma, L.S., Wang, T.J., 2004. Relationships between axisymmetric bending and buckling solutions of FGM circular plates based on third-order plate theory and classical plate theory. *Int. J. Solids Struct.* 41, 85-101.
- Martin, P.A., Richardson, J.D., Gray, L.J., Berger, J.R., 2002. On Green's function for a three-dimensional exponentially graded elastic solid. *Proc. R. Soc. London A* 458, 1931-1947.
- Nicotra, V., Podio Guidugli, P., Tiero, A., 1999. Exact equilibrium solutions for linearly elastic plate-like bodies. *J. Elast.* 56, 231-245.
- Plevako, V.P., 1971. On the theory of elasticity of inhomogeneous media. *J. Appl. Math. Mech.* 35, 806-813 (10.1016/0021-8928(71)90078-5).
- Reddy, J.N., 2000. Analysis of functionally graded plates. *Int. J. Num. Meth. Eng.* 47, 663-684.
- Reddy, J.N., Cheng, Z.-Q., 2001. Three-dimensional thermomechanical deformations of functionally graded rectangular plates. *Eur. J. Mech. A-Solid.* 20, 841-855.
- Reddy, J.N., Wang, C.M., Kitipornchai, S., 1999. Axisymmetric bending of functionally graded circular and annular plates. *Eur. J. Mech. A-Solid.* 18, 185-199.
- Reiter, T., Dvorak, G.J., Tvergaard, V., 1997. Micromechanical models for graded composite materials. *J. Mech. Phys. Solids* 45, 1281-1302.
- Sburlati, R., 2009. Three-dimensional analytical solution for an axisymmetric biharmonic problem. *J. Elast.* 95, 79-97.
- Sneddon, I.N., 1966. *Mixed boundary value problems in potential theory*, John Wiley and Sons, New York.
- Suresh, S., 2001. Graded materials for resistance to contact deformation and damage. *Science* 292, 2447-2451.
- Vel, S.S., Batra, R.C., 2003. Three-dimensional analysis of transient thermal stresses in functionally graded plates. *Int. J. Solids Struct.* 40, 7181-7196 (10.1016/S0020-7683(03)00361-5).
- Watson, G.N., 1966. *A treatise on the theory of Bessel Functions*, Cambridge Mathematical Library, Cambridge University Press, Cambridge.
- Yin, H.M., Sun, L.Z., Paulino, G.H., 2004. Micromechanics-based elastic model for functionally graded materials with particle interactions. *Acta Mater.* 52, 3535-3543.

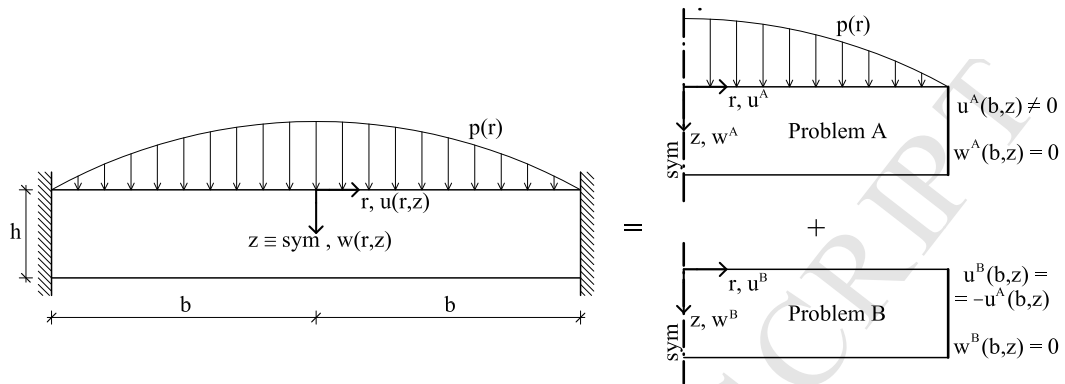


Figure 1: Schematic of the boundary value problem and the strategy of solution by superposition.

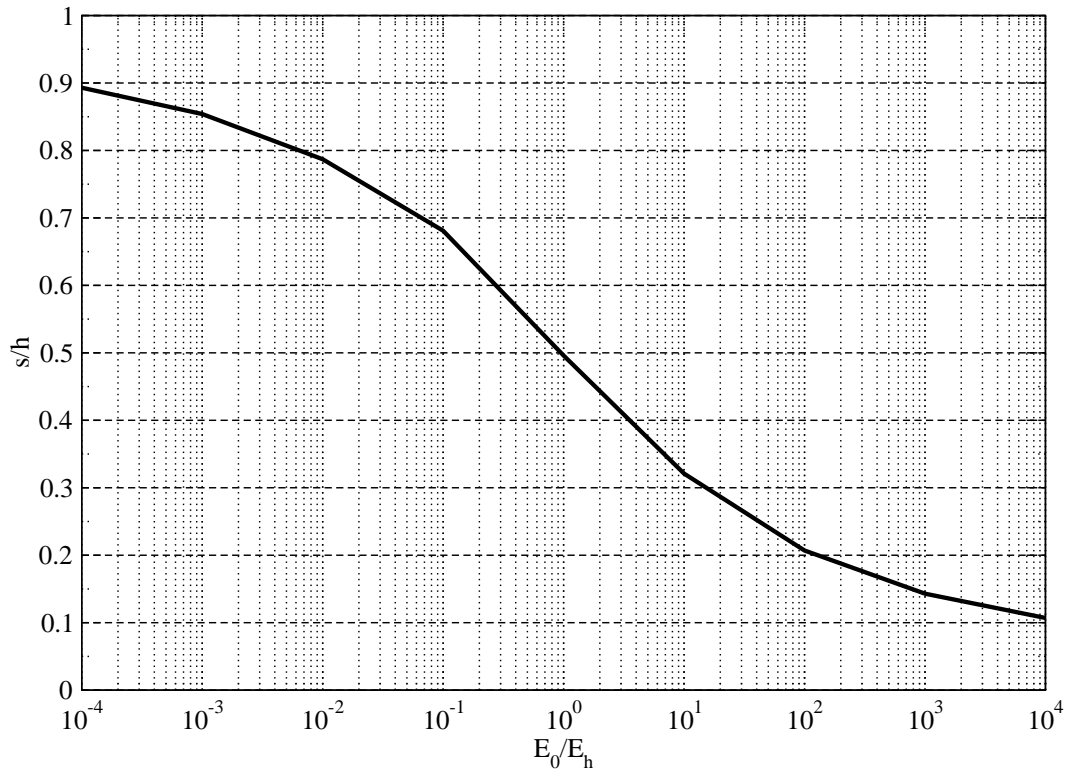


Figure 2: Position of the neutral plane as a function of the heterogeneity.

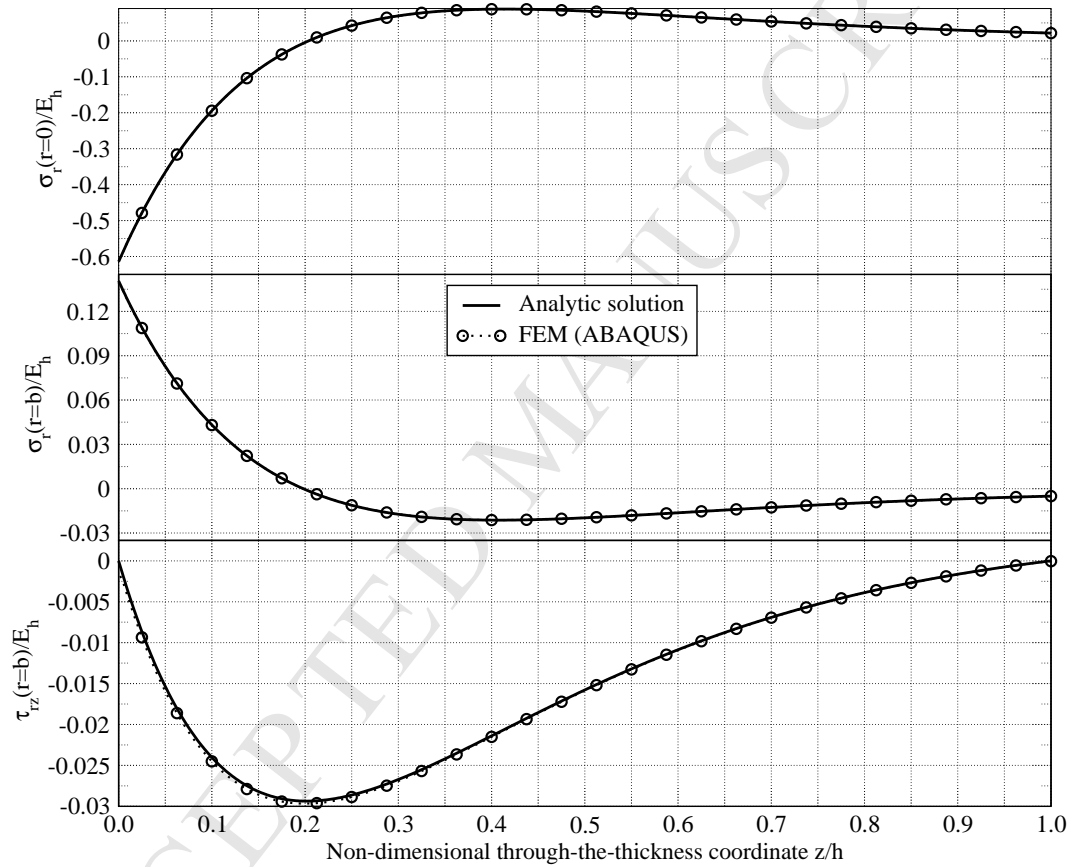


Figure 3: Problem A — comparison between FEM and analytic solutions in terms of the radial and shear stresses at the centre and on the mantle.

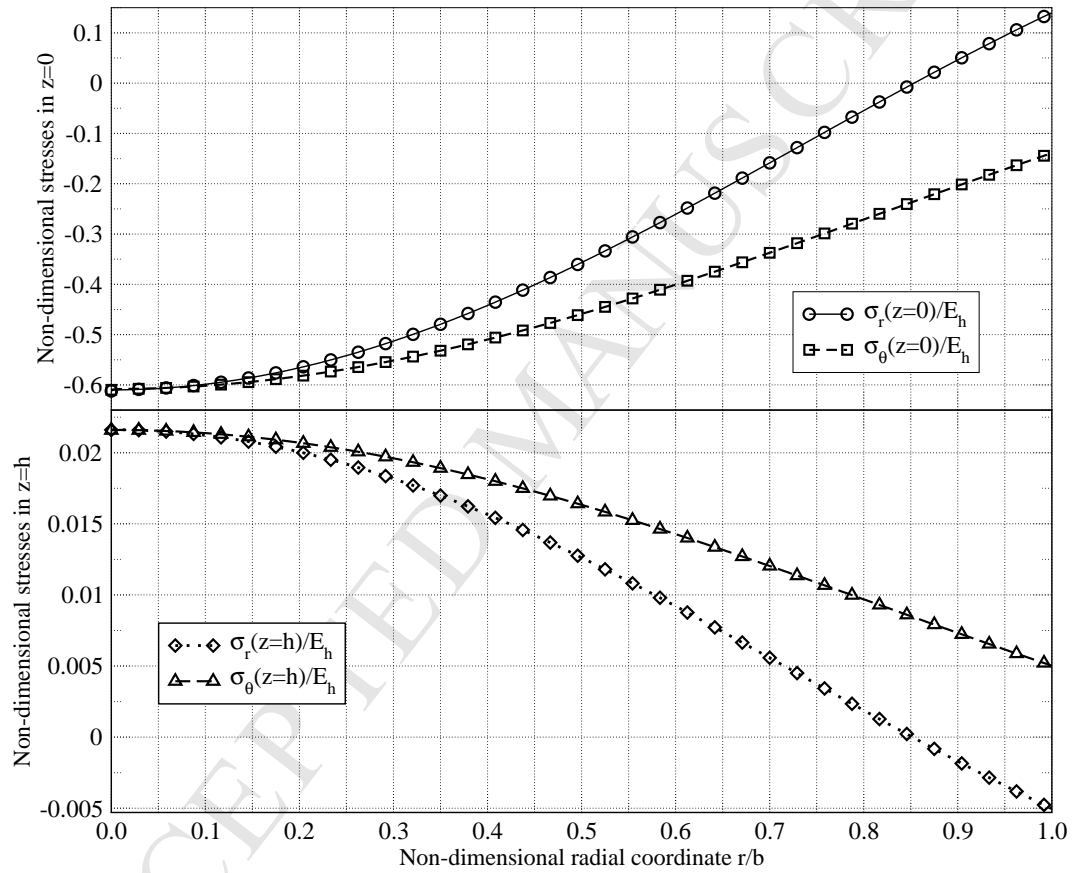


Figure 4: Problem A — radial and circumferential stresses on the ends.

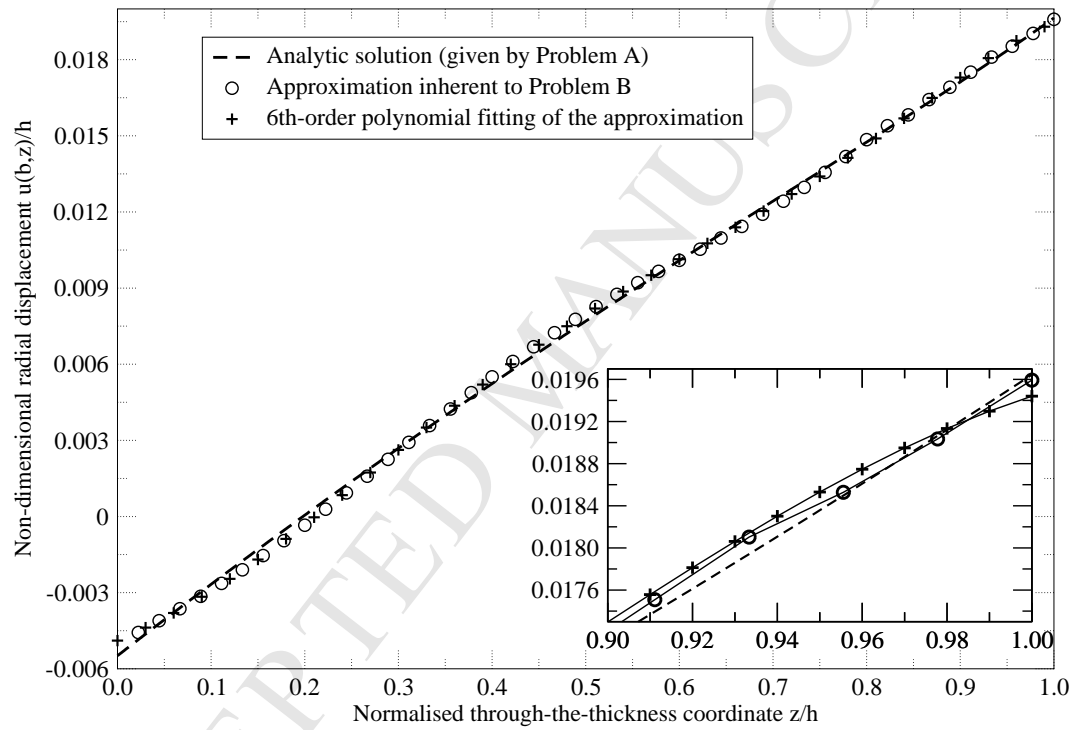


Figure 5: Comparison between $u^A(b, z)$ given by the Problem A, its approximation employed within the Problem B, and a 6th-order polynomial fitting of the latter.

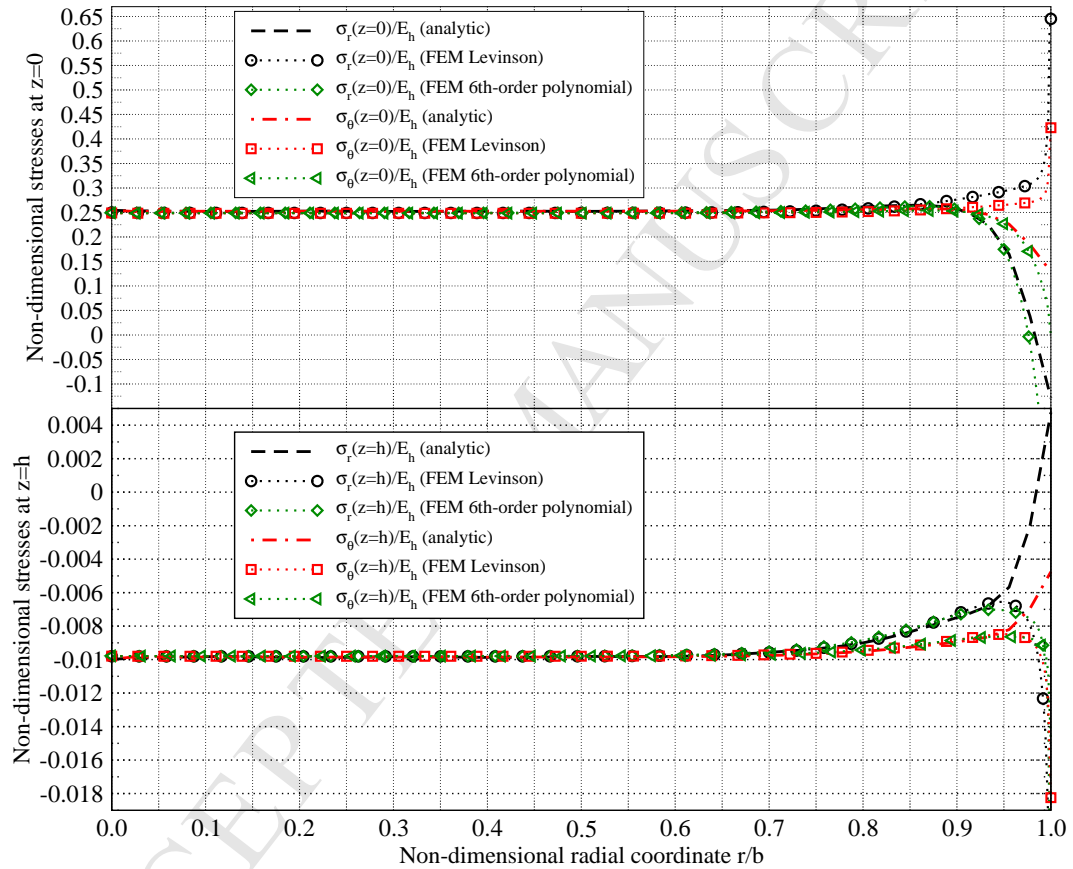


Figure 6: *Problem B* — comparison between *FEM* and analytic solutions in terms of the radial and circumferential stresses on the ends.

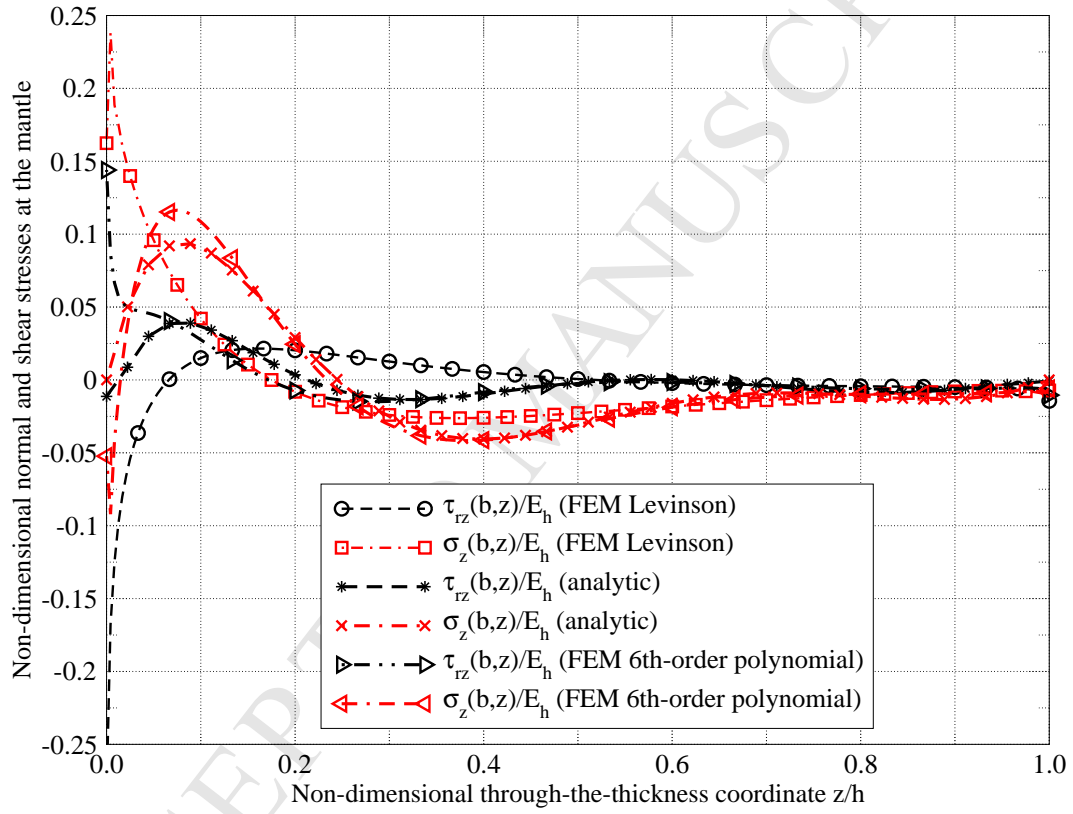


Figure 7: Problem B — comparison between FEM and analytic solutions in terms of normal and shear stresses on the mantle.

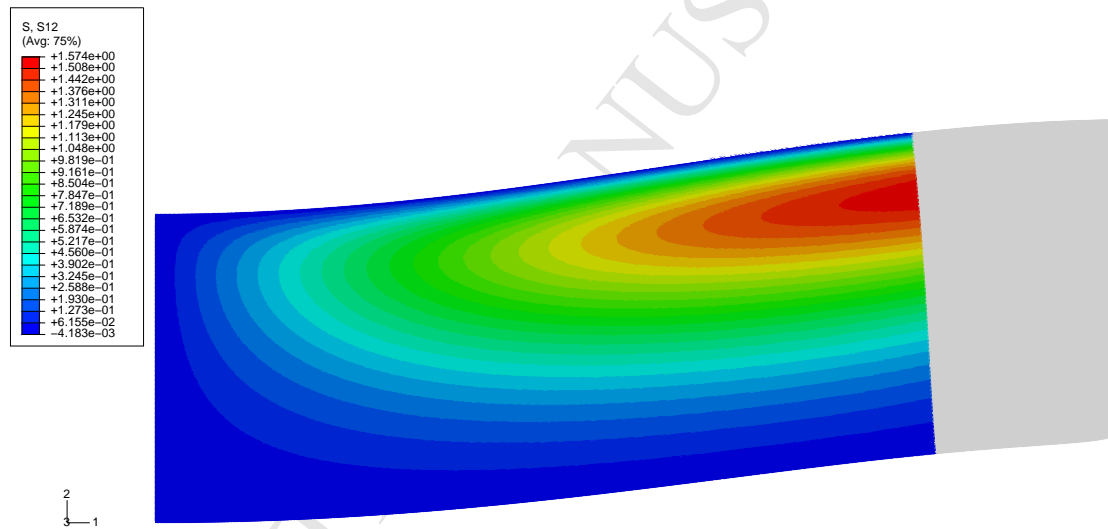


Figure 8: *Global problem* — contour of the shear stress on the 10 times amplified deformed shape.

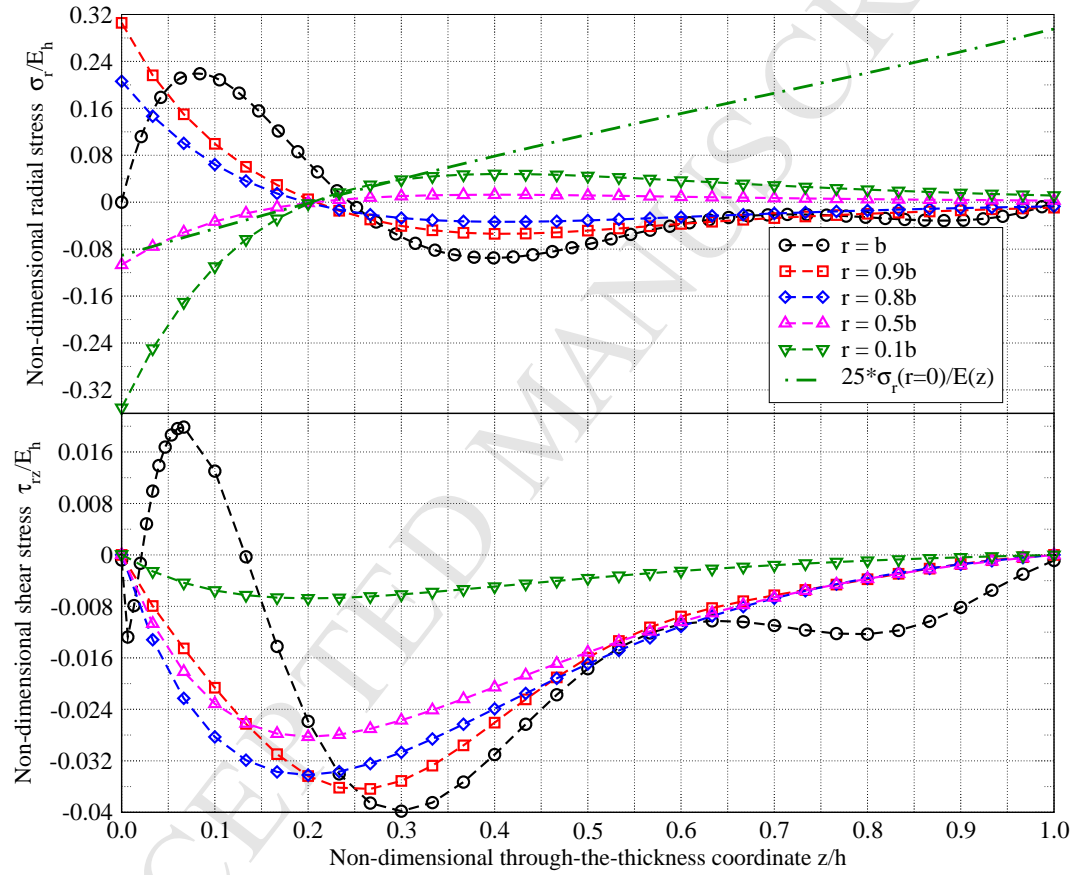


Figure 9: Global problem — analytic solution in terms of the radial and shear stresses.

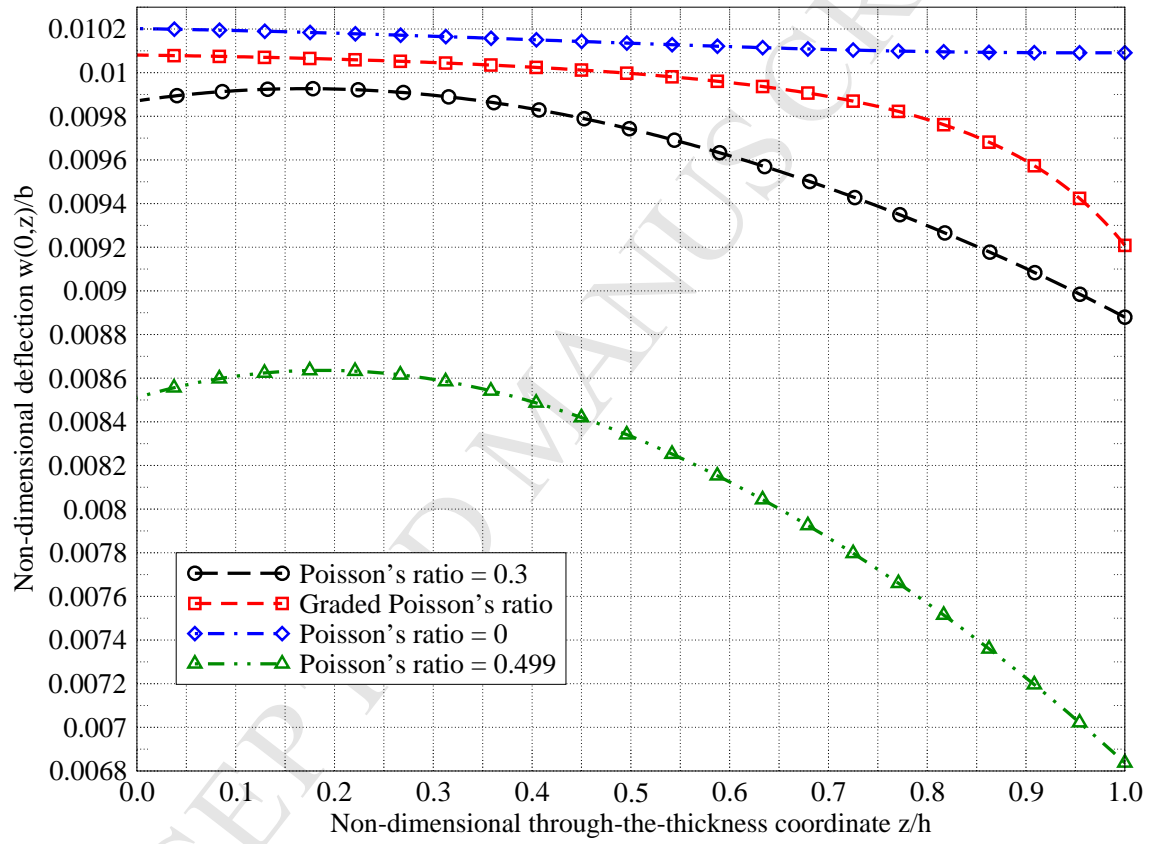


Figure 10: *Global problem — FEM solution in terms of the deflection at the centre, $w(0, z)/b$, also for the case of graded Poisson's ratio.*

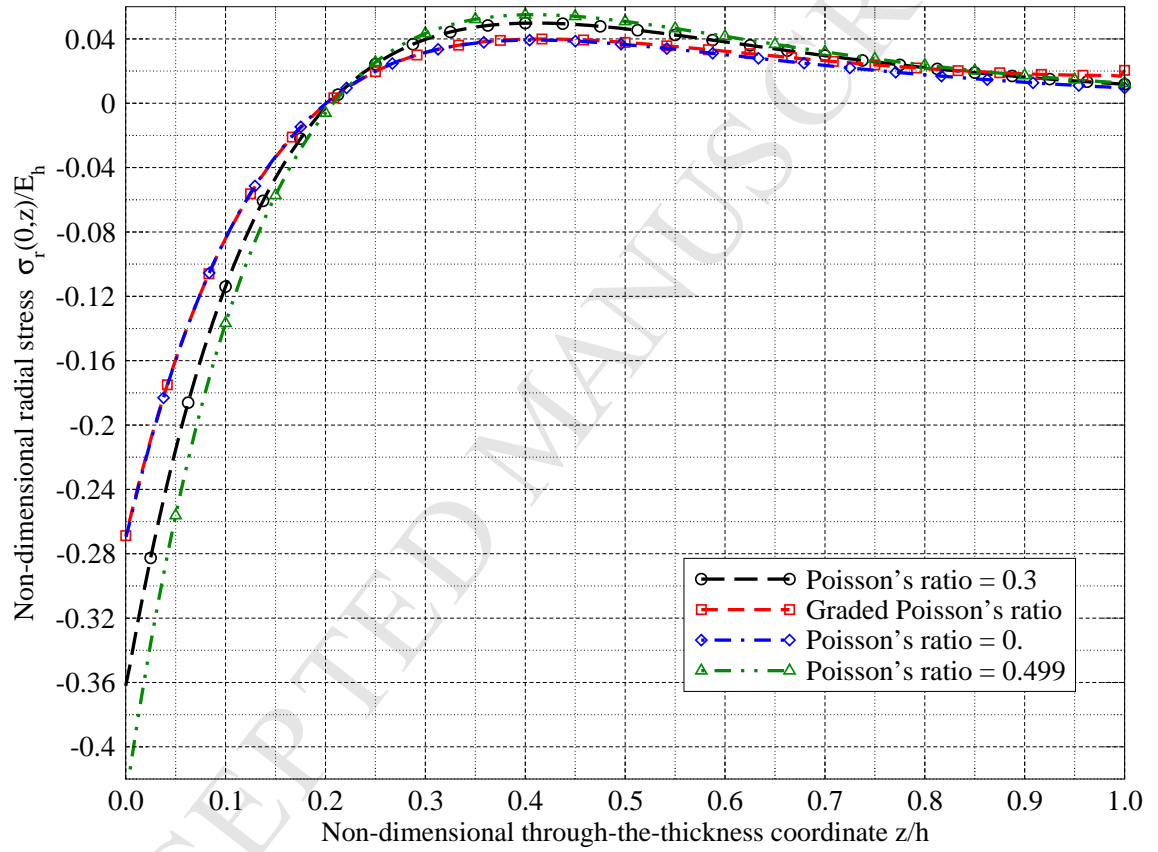


Figure 11: Global problem — FEM solution in terms of the radial stress at the centre, $\sigma_r(0, z)$, also for the case of graded Poisson's ratio.